MOLECULAR AND CELLULAR BIOLOGY, July 2000, p. 4708–4723 Vol. 20, No. 13
0270-7306/00/$04.00+0


# Cross Talk of pp125$^{FAK}$ and pp59$^{Lyn}$ Non-Receptor Tyrosine Kinases to Insulin-Mimetic Signaling in Adipocytes

GÜNTER MÜLLER,* SUSANNE WIED, AND WENDELIN FRICK

*Aventis Pharma Deutschland GmbH, 65926 Frankfurt am Main, Germany*

Received 31 January 2000/Returned for modification 20 March 2000/Accepted 12 April 2000

**Signaling molecules downstream from the insulin receptor, such as the insulin receptor substrate protein 1 (IRS-1), are also activated by other receptor tyrosine kinases. Here we demonstrate that the non-receptor tyrosine kinases, focal adhesion kinase pp125$^{FAK}$ and Src-class kinase pp59$^{Lyn}$, after insulin-independent activation by phosphoinositolglycans (PIG), can cross talk to metabolic insulin signaling in rat and 3T3-L1 adipocytes. Introduction by electroporation of neutralizing antibodies against pp59$^{Lyn}$ and pp125$^{FAK}$ into isolated rat adipocytes blocked IRS-1 tyrosine phosphorylation in response to PIG but not insulin. Introduction of peptides encompassing either the major autophosphorylation site of pp125$^{FAK}$, tyrosine 397, or its regulatory loop with the twin tyrosines 576 and 577 inhibited PIG-induced IRS-1 tyrosine phosphorylation and glucose transport. PIG-induced pp59$^{Lyn}$ kinase activation and pp125$^{FAK}$ tyrosine phosphorylation were impaired by the former and latter peptide, respectively. Up-regulation of pp125$^{FAK}$ by integrin clustering diminished PIG-induced IRS-1 tyrosine phosphorylation and glucose transport in nonadherent but not adherent adipocytes. In conclusion, PIG induced IRS-1 tyrosine phosphorylation by causing (integrin antagonized) recruitment of IRS-1 and pp59$^{Lyn}$ to the common signaling platform molecule pp125$^{FAK}$, where cross talk of PIG-like structures and extracellular matrix proteins to metabolic insulin signaling may converge, possibly for the integration of the demands of glucose metabolism and cell architecture.**

Multiple downstream effectors of insulin action are shared in common by many receptor tyrosine kinases. This necessitates the existence of mechanisms for incorporating specificity at each step in the insulin signal transduction pathway, starting at the receptor and receptor substrate levels (16). Integration of signals generated by the well-known cross talk of the insulin receptor to different types of non-insulin receptor tyrosine kinases (e.g., insulin-like growth factor 1 receptor [IGF-1R]) or of the latter (e.g., platelet-derived growth factor receptor [PDGF-R]) to the insulin receptor substrate (IRS) proteins may contribute to the specificity of insulin action. Upon tyrosine phosphorylation, IRS proteins provide a common interface for the activated receptor and various downstream (Src homology 2 domain [SH2] containing) signaling proteins, including phosphatidylinositol-3′-kinase (PI 3K), p55$^{PIK}$, Grb-2, SHP2, Nck, and Crk (67, 71, 72).

Specificity of insulin action may also be determined by the external environment of the cells mediated through signal cross talk from integrins. Integrins, transmembrane proteins expressed in most tissues, including insulin-sensitive adipose and muscle cells, bind to particular extracellular matrix proteins. The key biological functions of integrins, including cell migration and adhesion, are mediated in part by focal adhesion kinase, pp125$^{FAK}$ (2, 8). There is evidence that signaling pathways initiated by integrins synergize functionally with those triggered by growth factors (32, 55). Recent data imply that insulin potently augments $\alpha_5\beta_1$-integrin-mediated cell adhesion of insulin receptor-expressing CHO cells, while signaling via this integrin in turn enhances insulin receptor kinase activity and tyrosine phosphorylation and formation of complexes containing IRS-1 and PI 3K (15). The latter findings were extended to isolated rat adipocytes for artificial clustering of $\alpha_5\beta_1$-integrin (14). Thus, the insulin receptor may act synergistically with integrins to enhance cell adhesion, and, vice versa, the extracellular matrix surrounding the cell may influence signaling specificity by the insulin receptor.

A signaling pathway which also might sense information from the cellular environment or extracellular proteins and cross talk to various signal transduction cascades, such as insulin signaling, but is less well understood than the integrin system, emerges from glycosylphosphatidylinositol-anchored plasma membrane proteins (GPI proteins). The protein moiety of GPI proteins is attached to the extracellular face of the plasma membrane via a covalently attached glycolipid of the glycosylphosphatidylinositol (GPI) type that is embedded in the outer leaflet of the phospholipid bilayer (42). Two modes of initiation of signaling events through GPI proteins have been described so far. (i) Cross-linking of certain GPI proteins with antibodies in T cells and neutrophils elicits cell-specific responses via activation of non-receptor tyrosine kinases which are associated with the inner leaflet of the plasma membrane via their fatty acyl chains and form together with GPI proteins so-called glycolipid-enriched detergent-insoluble raft domains within the plasma membrane (5, 51, 56, 58, 59). (ii) Lipolytic cleavage of the GPI anchor of certain GPI proteins by a GPI-specific phospholipase C induces a range of insulin-mimetic metabolic effects in insulin-responsive cells (30, 35). The molecular mechanism(s) for signal transmission from GPI proteins via the plasma membrane to intracellular signaling cascades has not been elucidated for either mode; however, it has been linked to the generation of soluble phosphoinositolglycan (PIG) molecules in case of phospholipase C action (64).

PIG molecules represent the polar core glycan head groups of free GPI lipids or GPI protein membrane anchors. They consist of a cyclic phosphoinositol moiety coupled to nonacetylated glucosamine and an additional glycan structure, which in case of GPI protein membrane anchors, is built from three mannose residues in typical glycosidic linkages followed by a phosphodiester bridge to the terminal ethanolamine residue

* Corresponding author. Mailing address: Aventis Pharma Deutschland GmbH, DG Metabolic Diseases, Bldg. H825, 65926 Frankfurt am Main, Germany. Phone: 4969-305-4271. Fax: 4969-305-81767. E-mail: Guenter.Mueller@aventis.com.

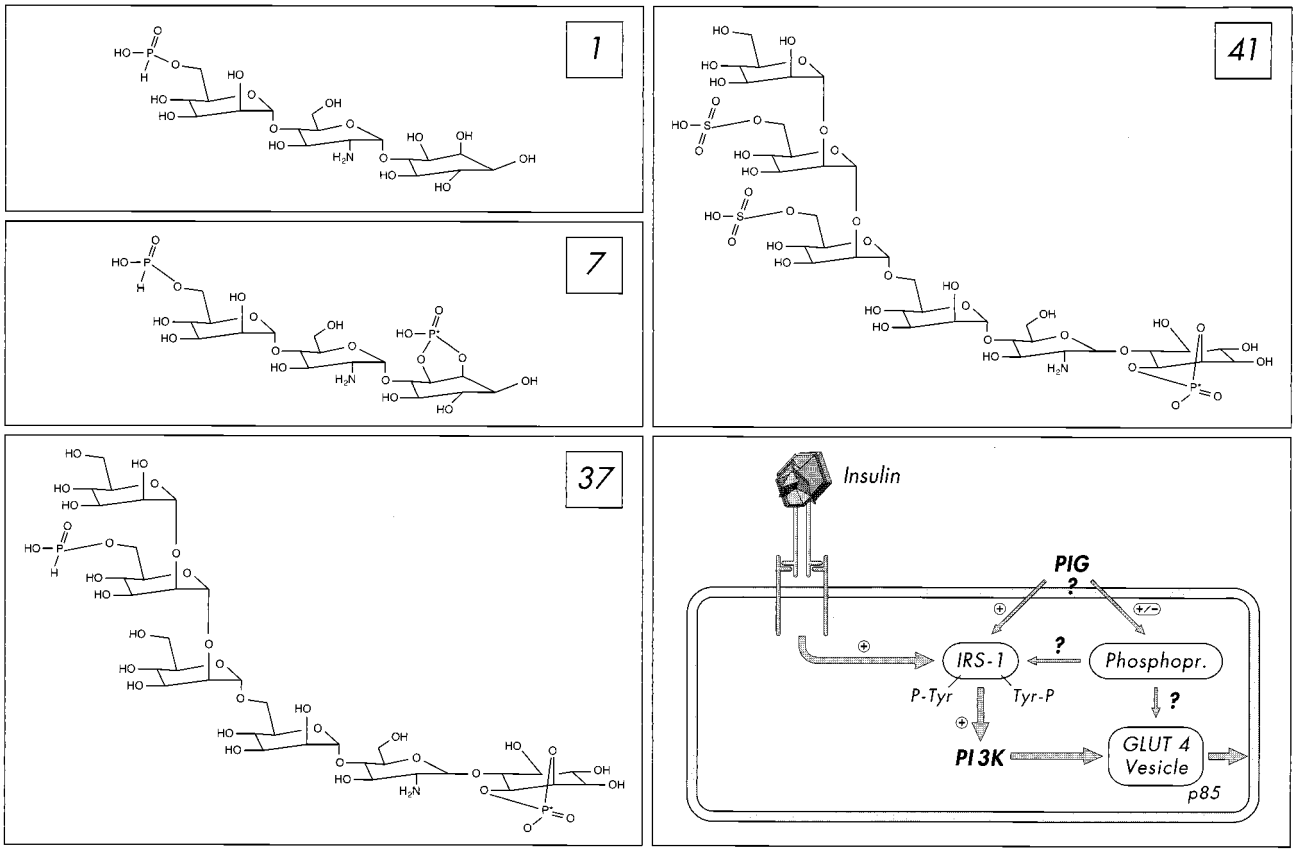


FIG. 1. Structure of the PIG compounds 1, 7, 37, and 41 (with the activity-determining phosphate moiety marked by an asterisk) and their mode of action in fat and muscle cells according to references 12 and 22 (also see the introduction). PIG compounds induce tyrosine phosphorylation of IRS proteins and their association with PI 3K, which is thereby activated, as does insulin by stimulating the insulin receptor tyrosine kinase. Operation of the IRS-1–PI 3K pathway (and possibly membrane association of the regulatory p85 subunit of PI 3K) is a prerequisite for fusion of GLUT4-containing vesicles with the plasma membrane, the so-called GLUT4 translocation, but may not be sufficient (also see Discussion). In addition, PIG compounds modulate the phosphorylation state of a number of phosphoproteins, which are not affected by insulin (22), but may be required for PIG-dependent GLUT4 translocation.

(20, 34, 36). During the past few years, we have demonstrated that chemically synthesized complete PIG molecules (Fig. 1) mimic a number of metabolic insulin effects (e.g., stimulation of glucose transport and nonoxidative glucose metabolism) in normal and insulin-resistant isolated fat and muscle cells at the micromolar range to up to the maximal insulin response (11). The complete glycan core structure (three mannose residues plus glucosamine) of typical GPI protein membrane anchors including a mannose side chain and the inositol(cyclic)phosphate moiety (Fig. 1) is required for maximal insulin-mimetic activity of PIG compounds, with some variations possible with regard to the type of residues coupled to the terminal mannose or inositol as well as the type of linkages involved (12). This potent insulin-mimetic metabolic activity of PIG compounds is not accompanied by stimulation of the insulin receptor tyrosine kinase; however, it correlates with dramatic tyrosine phosphorylation of IRS-1 as well as activation of PI 3K and its downstream-located cascade (12, 22, 39, 40). Thus, PIG compounds seem to mimic metabolic insulin action by insulin receptor-independent activation of the IRS-PI 3K pathway and thus circumvent defects at the level of the insulin receptor in muscle and adipose tissue (Fig. 1), which may represent (in part) the molecular basis for peripheral insulin resistance, the hallmark of non-insulin-dependent diabetes mellitus (28).

The present study was performed to identify the tyrosine kinase(s) responsible for PIG-dependent IRS phosphorylation and to characterize the upstream-located signaling cascade. We found that insulin-mimetic signaling by PIG compounds depends on activation and direct interaction of the $pp59^{Lyn}$ and $pp125^{FAK}$ non-receptor tyrosine kinases, which is antagonized by integrin engagement. This raises the possibility for cross talk of a GPI protein-mediated signal transduction cascade to metabolic insulin signaling via components of the cell adhesion pathway.

## MATERIALS AND METHODS

**Materials.** [$\gamma$-$^{32}$P]ATP (6,000 Ci/mmol) and 2-deoxy-D-[2,6-$^{3}$H]glucose (60 Ci/mmol) were bought from NEN/DuPont (Bad Homburg, Germany). PIG 41, 37, 45, 7, and 1 and recombinant human insulin were made available by the Departments of Medicinal Chemistry and Pharma Synthesis of Aventis Pharma (Frankfurt am Main, Germany). Recombinant human IRS-1 was delivered by Upstate Biotechnology (Lake Placid, N.Y.). $pp125^{FAK}$ (amino acids [aa] 385 to 405) Src docking site wild-type (Y397) peptide and mutant (F397) control peptide and $pp125^{FAK}$ (aa 368 to 388) control peptide, $pp125^{FAK}$ (aa 568 to 582) regulatory loop wild-type (Y576, Y577) peptide and mutant (F576, F577) control peptide, GRGDSP peptide, and GRADSP peptide were synthesized by Biotrend (Cologne, Germany). Human plasma fibronectin, rat plasma vitronectin, and poly-L-lysine were purchased from Sigma (Deisenhofen, Germany). Neutralizing anti-$pp59^{Lyn}$ and anti-$pp125^{FAK}$ antibodies were prepared in our laboratory by immunizing rabbits with the recombinant (insect cells) catalytic SH1 of human $pp59^{Lyn}$ comprising aa 217 to 512 and catalytic domain of chicken $pp125^{FAK}$ comprising aa 354 to 625, respectively, fused to amino-terminal glutathione *S*-transferase tags. Monoclonal antibodies against $pp59^{Lyn}$ (clone 42), paxillin

(clone 165), and pp125$^{FAK}$ (clone 77) for immunoprecipitation were obtained from Transduction Laboratories (Lexington, Ky.). Monoclonal antiphosphotyrosine antibody (clone 4G10) for immunoblotting was purchased from Upstate Biotechnology. Anti-IRS-1 antibody for immunoprecipitation raised in rabbits against total human recombinant (insect cells) IRS-1 (purified by gel filtration) was provided by Biotrend. Anti-IRS-1 antibody for immunoblotting raised in rabbits against a synthetic peptide corresponding to the carboxy-terminal sequence comprising aa 1223 to 1235 of rat IRS-1 was a kind gift of Suzanne Dalle (Humboldt University, Berlin, Germany). Monoclonal anti-$\beta_1$-integrin antibody (clone K20) for clustering was bought from Immunotech (San Francisco, Calif.). Monoclonal anti-$\beta_3$-integrin antibody for clustering (clone F11) was delivered by PharMingen (Heidelberg, Germany). Polyclonal antirat immunoglobulin G (IgG) (whole molecule) from rabbit (used as nonimmune IgG) was bought from Sigma (Deisenhofen, Germany). Materials for cell culture (including sera) were obtained from Gibco/BRL (Eggenstein/Leopoldshafen, Germany). Antibiotics and proteinase inhibitors were from Roche Molecular Biochemicals (Mannheim, Germany). Detergents were bought from Calbiochem (Bad Soden, Germany). All other chemicals were provided by Merck (Darmstadt, Germany) unless indicated otherwise.

**Preparation and stimulation of isolated rat adipocytes with insulin or PIG.** Adipocytes from epididymal fat pads of male Wistar rats prepared as described previously (39) were suspended in buffer S [Dulbecco's minimal essential medium (DMEM) containing 5 mM glucose, 0.5 mM sodium pyruvate, 4 mM L-glutamine, 200 nM 1-methyl-2-(phenylethyl)adenosine (PIA), 100 μg of gentamicin per ml, 1% bovine serum albumin (BSA), and 25 mM HEPES-KOH (pH 7.4)] at 5% cytocrit (corresponding to about $7 \times 10^5$ cells/ml). For determination of the packed cell volume, small aliquots of the cell suspension were aspirated into capillary hematocrit tubes and centrifuged for 90 s in a microhematocrit centrifuge in order to measure the fractional occupation of the suspension by the adipocytes (cytocrit). A 20-ml portion of the (electroporated) adipocyte suspension (5% cytocrit) was added to 20 ml of buffer S containing PIG or human insulin as indicated. Incubations (20 min, 37°C) were performed under 5% $CO_2$ in 200-ml polyethylene vials with shaking at 110 cycles/min and with a stroke length of 3.5 cm.

**Preparation and stimulation of adherent 3T3-L1 adipocytes with insulin or PIG.** 3T3-L1 fibroblasts were seeded in 12-well (60,000 cells/well) plates and maintained in DMEM (high glucose) plus 10% fetal bovine serum (FBS), 5 mM L-glutamine, and 2% BSA. Following 3 days at 100% confluence, differentiation was initiated by the addition of DMEM containing 10% FBS, 400 nM human insulin, 1 μM dexamethasone, and 1 mM isobutylmethylxanthine (Sigma, Deisenhofen, Germany). Three days later, the medium was replaced with DMEM plus 10% FBS and 100 nM insulin. After an additional 2 days, the medium was changed to DMEM (low glucose) plus 10% FBS. Adipocytes were used 5 to 12 days after completion of the differentiation protocol, when more than 85% of the cells expressed the adipocyte phenotype. Prior to experiments, the cells were rinsed two times with low serum medium (DMEM containing 5 mM glucose, 0.5% BSA, 0.1% FBS, 25 mM HEPES [pH 7.4] 10 mM glutamine, 100 U of streptomycin or penicillin per ml) and then incubated (12 to 14 h) in this medium and finally washed twice with phosphate-buffered saline (PBS) containing 2 mM sodium pyruvate prior to incubation (30 min, 37°C) with PIG or insulin as indicated in 4 ml of buffer S.

**Preparation and stimulation of nonadherent 3T3-L1 adipocytes with insulin or PIG.** Adherent 3T3-L1 adipocytes were serum starved for 12 h in a mixture of serum-free DMEM, 10 mM glutamine, 0.5% BSA, and 50 U of streptomycin or penicillin per ml; thereafter washed twice with PBS containing 1 mM EDTA; and then removed gently from the dishes by using a rubber policeman. After being washed once in PBS, the cells were maintained in suspension (30 min, 37°C) in 4 ml of PBS containing 5 mM glucose, 1% BSA, and 200 nM PIA before the addition of PIG or insulin as indicated and further incubation (30 min, 37°C).

**Attachment of 3T3-L1 adipocytes to fibronectin-coated dishes.** Cell culture dishes (12-well plates) were coated (4°C, overnight) with fibronectin (10 μg/ml) or poly-L-lysine (10 μg/ml) together with vitronectin (2 μg/ml) in PBS containing 2.7 mM KCl, 6.5 mM $Na_2HPO_4$, and 1.5 mM $KH_2PO_4$ (pH 7.4), blocked (1 h) with 0.1% BSA in PBS, and then dried (1 h, 37°C) prior to plating of the cells. Confluent 3T3-L1 adipocytes were serum starved for 12 h in serum-free DMEM, 10 mM glutamine, 0.5% BSA, and 50 U of streptomycin-penicillin per ml and then detached by adding EDTA-trypsin (0.05 mM, 0.025%). The detached adipocytes were washed three times with PBS containing 1% BSA and then held in suspension (30 min, 37°C) in 4 ml of buffer S prior to addition of PIG or insulin as indicated. After incubation (10 min, 37°C), the cells were replated on dishes coated with fibronectin or poly-L-lysine in the absence or presence of 25 μg of peptide per ml as indicated and further incubated (20 min, 37°C) under 5% $CO_2$.

**Electroporation of isolated rat adipocytes.** A 0.4-ml portion of buffer E (4.74 mM NaCl, 118 mM KCl, 0.38 mM $CaCl_2$, 1 mM EGTA, 1.19 mM $MgSO_4$, 1.19 mM $KH_2PO_4$, 25 mg of BSA per ml, 3 mM sodium pyruvate, 25 mM HEPES-KOH, pH 7.4) was placed in a 0.4-cm gap-width electroporation cuvette (Bio-Rad, Munich, Germany) together with the antibodies or peptides. A 0.4-ml portion of the adipocyte suspension (50% cytocrit in buffer E) was added to each cuvette and gently mixed. Electroporation was performed with a Gene Pulser Transfection Apparatus (Bio-Rad), which was set at a capacitance of 25 μF and voltage of 800 V (2 kV/cm), at 25°C for six shocks (46, 57). After the third treatment, the adipocyte suspension was gently stirred with a plastic stick, and the electric polarity was reversed. The time constant of electroporation was typically 0.6 ms during the final shock. Routinely, 4 ml of adipocyte suspension (25% cytocrit) was electroporated in five cuvettes. The time required for treatment of the five cuvettes was about 3 min. After electroporation, the cells from five electroporations were pooled and transferred to 50-ml polystyrene tubes (Falcon). After incubation (30 min, 37°C) in 5% $CO_2$–95% $O_2$, the cells were centrifuged ($200 \times g$, 1 min, swing-out rotor) and the infranatant was aspirated. Thereafter the cells were washed once with 40 ml of buffer S containing 4% BSA, suspended in 20 ml of buffer S, and then incubated (1 h, 37°C) under 5% $CO_2$ prior to stimulation with PIG or insulin (see above).

**Clustering of adipocytes.** Isolated rat adipocytes or nonadherent 3T3-L1 adipocytes were washed with buffer S containing 2% BSA and 2 mM pyruvate and then suspended in the same medium at 10% cytocrit. After 30 min of rest, the cells were incubated (30 min, 37°C) in the absence or presence of anti-$\beta_1$-integrin or anti-$\beta_3$-integrin antibody (4 μg/ml) together with plasma human fibronectin or poly-L-lysine (40 μg/ml) with or without further additions and then stimulated (20 min, 37°C) with PIG as indicated under 5% $CO_2$.

**Preparation of cell lysates.** Stimulated adherent or nonadherent 3T3-L1 cells were placed on ice and then washed twice with a mixture of 50 mM HEPES-KOH (pH 7.5), 150 mM NaCl, 1 mM $CaCl_2$, 1 mM $MgCl_2$, 10 mM EDTA, 10 mM glycerol-3-phosphate, 10 mM $Na_4P_2O_7$, 2 mM $Na_3VO_4$, 100 mM NaF (in the case of nonadherent cells by flotation [$200 \times g$, 2 min] and aspiration of the infranatant). Cells were solubilized in the above buffer containing 1% (vol/vol) Triton X-100, 0.1% sodium deoxycholate, 10% glycerol and protease inhibitors (20-μg/ml leupeptin, 10-μg/ml pepstatin A, 50-μg/ml aprotinin, 10 μM E-64, 0.5 mM phenylmethylsulfonylfluoride [PMSF] [lysis buffer]) for 30 min on ice (nonadherent cells) or by scraping with a Teflon policeman (adherent cells). Total lysates were centrifuged ($25{,}000 \times g$, 20 min, 18°C). The infranatant was aspirated, taking care to avoid contamination by the upper fat layer, and recentrifuged to obtain the defatted cell lysate. Stimulated normal or electroporated rat adipocytes were washed once with PBS containing 2 mM sodium pyruvate by flotation ($200 \times g$, 2 min) and aspiration of the infranatant and immediately homogenized in lysis buffer containing 4 mM benzamidine by 10 strokes/200 rpm in a medium-fitting Teflon-in-glass homogenizator (2-ml vessel volume) at 18°C. Defatted cell lysate was prepared as described above.

**Immunoprecipitation.** Defatted cell lysates (standardized for 5 to 10 μg of protein) were precleared (1 h, 4°C) with protein G or A-Sepharose (Pharmacia, Freiburg, Germany) and then supplemented with the appropriate antibodies (pp125$^{FAK}$, 2 μg/sample; IRS-1, 1:50 serum dilution; pp59$^{Lyn}$, 5 μg/sample; paxillin, 0.7 μg/sample) preadsorbed on protein G-Sepharose (monoclonal antibodies) or protein A-Sepharose (rabbit antibodies) in a total volume of 100 μl of lysis buffer. After incubation (4 h, 4°C, end-over-end rotation) and centrifugation ($13{,}000 \times g$, 2 min, 4°C), the collected immune complexes were washed twice with 1 ml each of immunoprecipitation buffer (50 mM HEPES-KOH [pH 7.4], 500 mM NaCl, 100 mM NaF, 10 mM EDTA, 10 mM $Na_4P_2O_7$, 1 mM $Na_3VO_4$) containing 1% NP-40 (omitted for sequential immunoprecipitation), and then twice with 1 ml each of immunoprecipitation buffer containing 150 mM NaCl and 0.1% NP-40 and once with 1 ml of immunoprecipitation buffer lacking salt and detergent and finally suspended in 50 μl of Laemmli buffer (2% sodium dodecyl sulfate [SDS], 5% 2-mercaptoethanol), heated (95°C, 2 min), and centrifuged. The supernatant samples were analyzed by SDS-polyacrylamide gel electrophoresis (PAGE; 4 to 12% Bis-Tris precast gel [pH 6.4], morpholinoethanesulfonic acid [MES]-SDS running buffer; Novex, San Diego, Calif.) under reducing conditions. For sequential immunoprecipitation, the supernatant samples (50 μl) were supplemented with 1 ml of immunoprecipitation buffer containing 1% NP-40 and 5 μl of anti-IRS-1 antiserum. After incubation (12 h, 4°C), 50 μl of protein A-Sepharose (100 mg/ml in immunoprecipitation buffer) was added, and the incubation continued (4 h, end-over-end rotation). The immune complexes were collected, washed, and processed for SDS-PAGE as described above.

**Immunoblotting.** Proteins were transferred to polyvinylidene difluoride membranes (Immobilon; Millipore, Eschborn, Germany). The blocked membrane was incubated (2 h, 25°C) with antibodies against pp125$^{FAK}$ (1:200), IRS-1 (1:500), or phosphotyrosine (2 μg/ml), washed (four times with Tris-buffered saline [TBS] containing 1% [vol/vol] NP-40 and 0.5% Tween 20, twice with TBS containing 0.5% Tween 20, and twice with TBS) and then incubated (1 h, 25°C) with the appropriate horseradish peroxidase-coupled detection (antimouse or antirabbit) antibodies (1:15,000 dilution; enhanced luminescence; Pierce, Rockford, Ill.) in TBS containing 5% (wt/vol) BSA, washed (five times with TBS containing 1% NP-40 and 0.5% Tween 20, three times with TBS containing 0.05% Tween 20), and finally processed with chemiluminescent reagents (Renaissance Chemiluminescence Detection System; NEN/DuPont, Bad Homburg, Germany) and subjected to phosphorimaging.

**Immune complex kinase assays.** pp59$^{Lyn}$ or pp125$^{FAK}$ immune complexes were washed in kinase buffer (50 mM HEPES-KOH [pH 7.4], 100 mM NaCl, 5 mM $MnCl_2$, 1 mM $MgCl_2$, 0.5 mM dithiothreitol [DTT], 1 mM $Na_3VO_4$), and then suspended in 50 μl of kinase buffer. The kinase reactions were started by addition of ATP (unlabeled or $^{32}$P-labeled; final concentrations: pp59$^{Lyn}$, 40 μM; 0.2 mCi/ml; pp125$^{FAK}$, 100 μM, 0.5 mCi/ml) and incubated (pp59$^{Lyn}$, 15 min; pp125$^{FAK}$, 3 min [22°C]) in the absence (autophosphorylation) or presence of recombinant human IRS-1 (0.3 μg) or heat-denatured (10 min, boiling waterbath) rabbit muscle enolase (1 μg; Sigma, Deisenhofen, Germany). Autophos-

TABLE 1. Inhibition of pp59$^{Lyn}$ by neutralizing antibody in the immune complex kinase assay[a]

| Antibody dilution | Phosphorylation (arbitrary units) | | |
|---|---|---|---|
| | Auto | Enolase | IRS-1 |
| None | 15,899 ± 1,756 | 2,974 ± 435 | 6,452 ± 855 |
| Anti-rat IgG (1:50) | 14,247 ± 1,530 | 3,012 ± 277 | 7,231 ± 1,034 |
| Anti-pp59$^{Lyn}$ | | | |
| 1:10,000 | 15,023 ± 1,980 | 3,189 ± 355 | 6,974 ± 893 |
| 1:2,000 | 13,577 ± 1,436 | 2,746 ± 301 | 4,760 ± 599 |
| 1:500 | 5,231 ± 965 | 1,235 ± 188 | 1,921 ± 266 |
| 1:100 | 1,930 ± 214 | 702 ± 87 | 1,213 ± 158 |
| 1:50 | 895 ± 101 | 254 ± 33 | 1,045 ± 213 |
| 1:25 | 799 ± 132 | 212 ± 45 | 823 ± 174 |

[a] pp59$^{Lyn}$ was immunoprecipitated with monoclonal anti-pp59$^{Lyn}$ antibody from defatted cell lysates (portions of 5 μg of protein) prepared from isolated rat adipocytes. The immune complexes were then incubated (30 min, 4°C) with neutralizing anti-pp59$^{Lyn}$ or anti-rat IgG antibody at various dilutions and subsequently subjected to kinase assay by incubation with [$^{32}$P]ATP in the absence (for autophosphorylation) or presence of denatured enolase or IRS-1. Total mixtures were separated by SDS-PAGE. Phosphorylated pp59$^{Lyn}$, enolase, or IRS-1 was quantitatively evaluated by phosphorimaging (arbitrary units). The experiment was repeated three times (mean ± standard deviation).

phorylation reactions were terminated by addition of 50 μl of ice-cold stop buffer (50 mM HEPES-KOH [pH 7.4], 150 mM NaCl, 100 mM ATP, 0.05% Triton X-100) and washing of the beads twice with 1 ml of stop buffer prior to addition of 20 μl of Laemmli buffer and boiling (95°C, 5 min). Substrate phosphorylation reactions were terminated by addition of 10 μl of fourfold-concentrated Laemmli buffer and boiling. The phosphoproteins were separated by SDS-PAGE (10% Bis-Tris resolving gel, MES-SDS running buffer) and analyzed by phosphorimaging directly (use of [$^{32}$P]ATP) or after immunoblotting with antiphosphotyrosine antibody (use of unlabeled ATP). Under these conditions, the kinase reactions were linear with time for the assay period.

**Glucose transport.** Glucose transport was assayed after two washing cycles of the cells with glucose-free and serum-free DMEM by using 2-deoxy-D-[2,6-$^{3}$H]glucose (50 μM, 0.33 μCi/ml; 20 min at 37°C) in the absence or presence of 20 μM cytochalasin B for isolated rat adipocytes and nonadherent 3T3-L1 adipocytes by using the oil-centrifugation method (39) and for adherent 3T3-L1 adipocytes by washing the cells twice with ice-cold PBS containing 5 mM D-glucose and subsequent addition of 0.2% SDS–0.1 N NaOH prior to liquid scintillation counting (61).

**Miscellaneous.** Protein concentration was determined by the bicinchoninic acid protein assay protocol from Pierce (Rockford, Ill.) with crystalline BSA as a standard. Phosphorimaging was performed with a Storm 860 PhosphorImager (Molecular Dynamics) and quantitatively evaluated with ImageQuant software (Molecular Dynamics). Differences in recovery in the amounts of immunoprecipitated protein during a specific experiment were corrected in each case (data on fold or percent stimulation) for the amount of protein actually applied to the gel by homologous immunoblotting. All of the results reported herein were confirmed by running independent experiments with different batches of adipocytes several times (as indicated in the figure legends), each with two to five parallel independent immunoprecipitation, kinase assay, and immunoblotting analyses.

## RESULTS

**Involvement of pp59$^{Lyn}$ in insulin-mimetic signaling by PIG in adipocytes.** Our previous studies unequivocally have demonstrated that insulin-mimetic signaling by PIG critically depends on insulin receptor-independent tyrosine phosphorylation of IRS-1, -2, and -3 (39, 40). Differential sensitivity of insulin and PIG stimulation of lipogenesis toward tyrosine kinase inhibitors (11) and the reported association of members of Src-class kinases with GPI proteins (see Introduction) led us to speculate on the involvement of non-receptor rather than receptor tyrosine kinases in PIG signaling (34). Furthermore, Lebrun and coworkers found that expression of a constitutive active pp60$^{Src}$ in 293 EBNA cells results in strong IRS-1 tyrosine phosphorylation (27). In addition, during an effort to identify new IRS-1 binding proteins by screening a mouse embryo expression library with recombinant [$^{32}$P]IRS-1, a specific association between IRS-1 and pp60$^{Fyn}$ via its SH2 domain and Tyr$^{895}$ and Tyr$^{1172}$ of IRS-1 was detected (60). These results suggested a role for Src-class kinases during insulin signaling. pp59$^{Lyn}$ kinase is the predominant Src-class kinase in isolated rat adipocytes (47) and was therefore selected as a candidate non-insulin receptor tyrosine kinase for PIG-dependent IRS phosphorylation.

We studied the participation of pp59$^{Lyn}$ in PIG signaling by using a polyclonal antibody raised against its kinase domain. The concentration-dependent inhibition of pp59$^{Lyn}$ activity by this antibody was demonstrated in an immune complex kinase assay with pp59$^{Lyn}$ immunoprecipitated from rat adipocytes (Table 1). A 1:50 dilution of the serum blocked more than 80% of pp59$^{Lyn}$ autophosphorylation as well as enolase and IRS-1 phosphorylation compared to an unrelated antibody. The anti-pp59$^{Lyn}$ antibodies used for neutralization as well as immunoprecipitation were highly specific, since they did not inhibit and precipitate (according to activity and protein, respectively), the closely related Src kinase family members pp60$^{Fyn}$ and pp60$^{Src}$ to any significant extent in in vitro kinase assays using the recombinant proteins (Table 2). The neutralizing antibody was introduced into isolated rat adipocytes by electroporation with high efficiency as shown by analysis of pp59$^{Lyn}$ autophosphor-

TABLE 2. Specificity of the antibodies used for neutralization and immunoprecipitation of pp59$^{Lyn}$ and pp125$^{FAK}$[a]

| Antibody | Response to recombinant kinase (concn of [$^{32}$P]enolase or [$^{32}$P]paxillin/kinase protein [% of maximum]) | | | | |
|---|---|---|---|---|---|
| | pp59$^{Lyn}$ | pp60$^{Fyn}$ | pp60$^{Src}$ | pp125$^{FAK}$ | pp116$^{PYK2}$ |
| None | 100 | 100 | 100 | 100 | 100 |
| Neutralizing | | | | | |
| Anti-pp59$^{Lyn}$ | 22 ± 8 | 93 ± 9 | 91 ± 5 | | |
| Anti-pp125$^{FAK}$ | 98 ± 4 | 95 ± 7 | 103 ± 6 | 30 ± 4 | 89 ± 6 |
| Immunoprecipitation | | | | | |
| Anti-pp59$^{Lyn}$ | 85 ± 9/92 ± 5 | 0/0 | 2 ± 1/3 ± 2 | | |
| Anti-pp125$^{FAK}$ | 0/0 | 0/3 ± 1 | 4 ± 3/0 | 78 ± 8/85 ± 6 | 6 ± 1/0 |

[a] Recombinant kinases (1 to 5 μg) were incubated (30 min, 4°C) in the absence or presence of neutralizing anti-pp59$^{Lyn}$ (1:50) or anti-pp125$^{FAK}$ (1:100) antibodies and then subjected to kinase assay by incubation with [$^{32}$P]ATP in the presence of denatured enolase (for pp59$^{Lyn}$, pp60$^{Fyn}$, or pp60$^{Src}$) or paxillin (for pp125$^{FAK}$ or pp116$^{PYK2}$). Alternatively, recombinant kinases (1 to 5 μg) were immunoprecipitated with monoclonal anti-pp59$^{Lyn}$ (5 μg/sample) or anti-pp125$^{FAK}$ (2 μg/sample) antibodies. The immune complexes were subjected to kinase assay (see above) or immunoblotted with corresponding antibodies to the different kinases. [$^{32}$P]enolase or [$^{32}$P]paxillin and immunoblotted kinase protein were quantitatively evaluated by phosphorimaging and set at 100% in a control incubation lacking antibody in each case. The experiment was repeated three times (mean ± standard deviation).

TABLE 3. Inhibition of pp59$^{Lyn}$ by neutralizing antibody in adipocytes[a]

| Antibody dilution | Phosphorylation (arbitrary units) | | |
|---|---|---|---|
| | Basal | PIG 41 | Insulin |
| None | 8,513 ± 1,112 | 94,672 ± 12,732 | 32,462 ± 4,244 |
| Anti-rat IgG (1:25) | 8,034 ± 1,034 | 91,207 ± 13,245 | 35,785 ± 4,890 |
| Anti-pp59$^{Lyn}$ | | | |
| 1:2,000 | 8,744 ± 1,055 | 85,992 ± 11,308 | 39,833 ± 4,067 |
| 1:500 | 7,231 ± 865 | 50,315 ± 7,855 | 23,121 ± 3,133 |
| 1:100 | 6,023 ± 762 | 37,312 ± 2,988 | 19,452 ± 2,629 |
| 1:50 | 5,149 ± 441 | 27,057 ± 3,562 | 10,038 ± 1,759 |
| 1:25 | 4,540 ± 331 | 23,560 ± 2,234 | 8,207 ± 1,552 |
| 1:10 | 4,267 ± 255 | 20,135 ± 2,433 | 7,064 ± 970 |

[a] Isolated rat adipocytes were electroporated with neutralizing anti-pp59$^{Lyn}$ or anti-rat IgG antibody at various dilutions and then incubated (15 min, 37°C) in the absence or presence of PIG 41 (3 μM) or human insulin (10 nM). pp59$^{Lyn}$ was immunoprecipitated with monoclonal anti-pp59$^{Lyn}$ antibody from defatted cell lysates and then immunoblotted with antiphosphotyrosine antibody. Autophosphorylated kinase was quantitatively evaluated by phosphorimaging (arbitrary units). The experiment was repeated twice (mean ± standard deviation).

ylation in the basal or insulin-stimulated state (Table 3). Basal and insulin-induced tyrosine phosphorylation of pp59$^{Lyn}$ were diminished during the 15-min incubation period in a serum concentration-dependent manner by up to 50 and 75%, respectively, compared to unrelated control antibody. The tyrosine phosphorylation left may be due to extrinsic pp59$^{Lyn}$ phosphorylating enzyme(s). A 1:25 dilution of the neutralizing antibody was used for analysis of IRS-1 tyrosine phosphorylation in electroporated rat adipocytes following incubation with increasing concentrations of PIG 41 or human insulin. Stimulation of IRS-1 tyrosine phosphorylation by PIG 41 was significantly impaired compared to that of the control antibody with regard to both maximal responsiveness (from 19.3- to 9.7-fold) and sensitivity (Fig. 2). In contrast, basal and insulin-dependent IRS-1 tyrosine phosphorylations were not significantly affected. These data represented a first indication that pp59$^{Lyn}$ mediates (directly or indirectly) PIG-induced, but not insulin-induced and basal, tyrosine phosphorylation of IRS-1.

We next studied with an immune complex kinase assay whether PIG compounds (of various structures and potencies) manage to activate pp59$^{Lyn}$ kinase in rat adipocytes. PIG 41 induced pp59$^{Lyn}$ autophosphorylation in a concentration-dependent fashion (at concentrations effective in stimulating glucose metabolism in adipocytes [12]) to up to 13.2-fold with effective concentrations for half-maximal activation ($EC_{50}$) of 0.24 μM. PIG 37 and 7 were significantly less potent, whereas PIG 1 was virtually inactive. The PIG-induced increase in pp59$^{Lyn}$ tyrosine phosphorylation was reduced by the neutralizing anti-pp59$^{Lyn}$ antibody in a concentration-dependent fashion by up to 75% compared to an unrelated antibody (Table 3), which correlated well with the anti-pp59$^{Lyn}$ antibody-mediated blockade of IRS-1 tyrosine phosphorylation in response to PIG 41 (Fig. 2). Interestingly, insulin also caused considerable activation of pp59$^{Lyn}$, although to a much lower degree (3.7-fold at 3 nM; Fig. 3A). The PIG- or insulin-induced autophosphorylation of pp59$^{Lyn}$ in rat adipocytes was accompanied by increased IRS-1 tyrosine phosphorylation irrespective of whether incorporation of radiolabeled phosphate into IRS-1 or antiphosphotyrosine immunoreactivity of IRS-1 was followed (Fig. 3B). The levels of effectiveness of the four PIG compounds with regard to both maximal responsiveness (fold-stim-

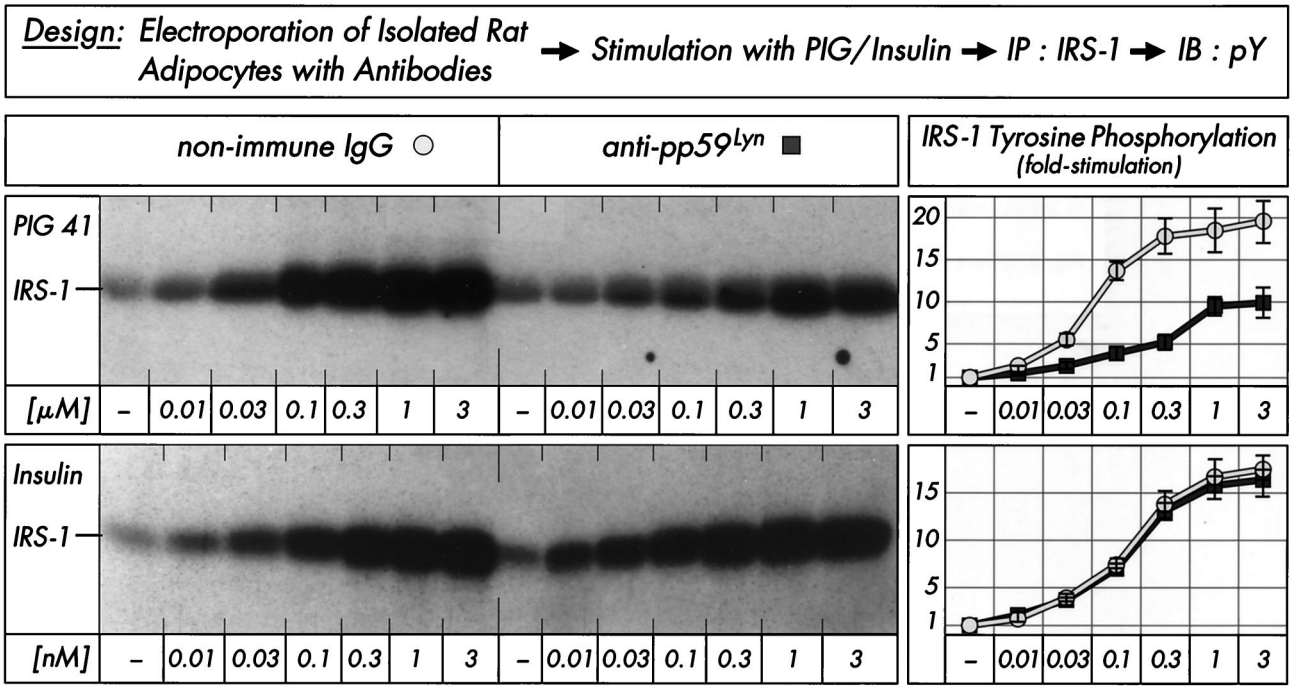


FIG. 2. Effect of anti-pp59$^{Lyn}$ antibody on PIG-induced IRS-1 tyrosine phosphorylation in adipocytes. Isolated rat adipocytes were electroporated with nonimmune IgG or neutralizing anti-pp59$^{Lyn}$ antibody (1:25) and then incubated in the absence or presence of increasing concentrations of PIG 41 or human insulin. IRS-1 was immunoprecipitated (IP) with anti-IRS-1 antibody from defatted cell lysates and then immunoblotted (IB) with antiphosphotyrosine antibody. Phosphorimages of a typical experiment are shown (left section) repeated four times with similar results. Quantitative evaluation is given as fold stimulation (mean ± standard deviation [right section]). Basal tyrosine phosphorylation is set at 1 in each case.

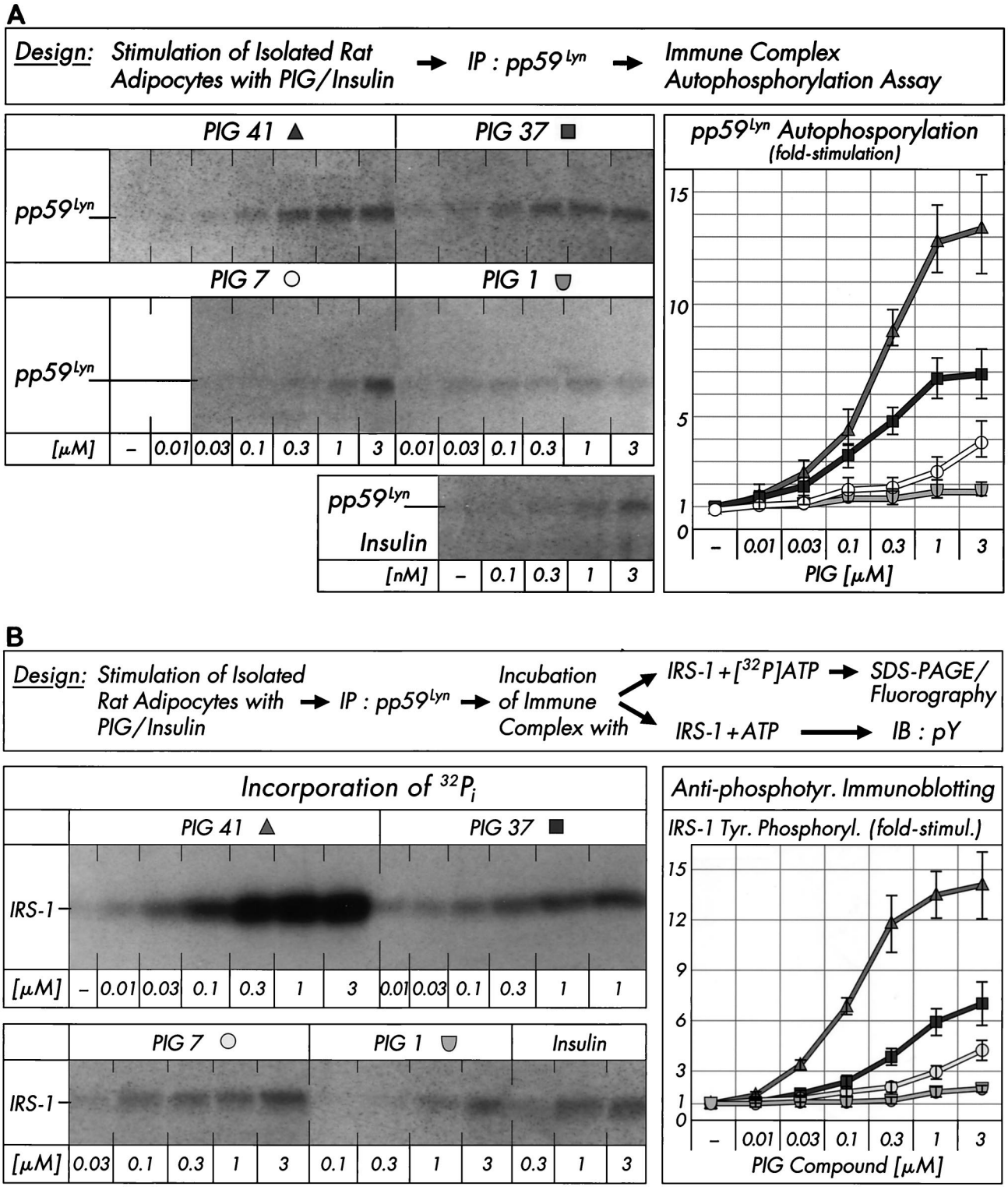


FIG. 3. Effect of PIG compounds on pp59$^{Lyn}$ activity. Isolated rat adipocytes were incubated in the absence or presence of increasing concentrations of PIG compounds or human insulin. pp59$^{Lyn}$ was immunoprecipitated (IP) with anti-pp59$^{Lyn}$ antibody from defatted cell lysates and then subjected to immune complex kinase assays for autophosphorylation by incubation with unlabeled ATP (A) or phosphorylation of recombinant human IRS-1 by incubation with either [$^{32}$P]ATP or unlabeled ATP (B). Phosphorimages of a typical experiment are shown (left sections) repeated three times with similar results. Basal pp59$^{Lyn}$ autophosphorylation and IRS-1 tyrosine phosphorylation were rather low and comparable to those observed in the presence of up to 0.01 μM PIG 37, 7, and 1 (which are shown instead of the basal phosphorylations only). Quantitative evaluation is given as fold stimulation (mean ± standard deviation [right sections]). Basal phosphorylation is set at 1 in each case. Insulin increased autophosphorylation of pp59$^{Lyn}$ and tyrosine phosphorylation of IRS-1 (according to antiphosphotyrosine immunoblotting [IB]), respectively, 1.6- to 1.4-fold at 0.3 nM, 2.2- to 2.7-fold at 1 nM, and 3.1- to 2.9-fold at 3 nM versus the basal level.

TABLE 4. Inhibition of pp125$^{FAK}$ by neutralizing antibody in the immune complex kinase assay and adipocytes[a]

| Parameter | Phosphorylation (% of basal) | | | | | |
|---|---|---|---|---|---|---|
| | Antirat IgG | | | Anti-pp125$^{FAK}$ | | |
| | Basal | PIG 41 | Insulin | Basal | PIG 41 | Insulin |
| Phosphorylation | | | | | | |
| Cell-free paxillin | 100 | | | 33 ± 8 | | |
| Cellular pp125$^{FAK}$ | 100 | 1,345 ± 210 | 576 ± 102 | 86 ± 10 | 711 ± 95 | 342 ± 48 |
| Cellular paxillin | 100 | 635 ± 102 | 289 ± 45 | 93 ± 7 | 295 ± 42 | 105 ± 18 |
| Cellular IRS-1 | 100 | 1,487 ± 255 | 1,753 ± 188 | 89 ± 5 | 804 ± 92 | 1,693 ± 140 |
| Glucose transport | 100 | 1,777 ± 142 | 1,896 ± 153 | 90 ± 8 | 925 ± 48 | 1,958 ± 166 |

[a] Defatted cell lysates from isolated rat adipocytes were incubated (30 min, 4°C) in portions (10 μg of protein) with neutralizing anti-pp125$^{FAK}$ or antirat IgG (IgG) antibody (1:100). After immunoprecipitation with monoclonal anti-pp125$^{FAK}$ antibody, the immune complexes were subjected to kinase assay by incubation with [$^{32}$P]ATP in the presence of paxillin. Total mixtures were separated by SDS-PAGE. Phosphorylated paxillin was quantitatively evaluated by phosphorimaging. Isolated rat adipocytes were electroporated with neutralizing anti-pp125$^{FAK}$ or antirat IgG antibody (1:50) and then incubated (15 min, 37°C) in the absence or presence of PIG 41 (3 μM) or human insulin (10 nM). pp125$^{FAK}$, paxillin, and IRS-1 were immunoprecipitated with the corresponding antibodies from defatted cell lysates and then immunoblotted with antiphosphotyrosine antibody. Phosphorylated proteins were quantitatively evaluated by phosphorimaging. Portions of the cells were assayed for 2-deoxyglucose transport. Basal values (incubation and electroporation with IgG) were set at 100% in each case. The experiment was repeated three times (mean ± standard deviation).

ulation) and sensitivity ($EC_{50}$) were similar for auto- and IRS-1 phosphorylation. The rankings of these PIG compounds in causing pp59$^{Lyn}$ and glucose transport activation in rat adipocytes are identical (12).

**Involvement of pp125$^{FAK}$ in insulin-mimetic signaling and action by PIG in adipocytes.** In many cell types, Src-class kinase family members are activated by the cytosolic focal adhesion kinase, pp125$^{FAK}$, which is involved in integrin signaling, cytoskeletal reorganization, and signal transduction by a number of growth factors (13, 48, 76). Recently it was found that in nonattached cells, insulin promotes pp125$^{FAK}$ phosphorylation and activation and pp125$^{FAK}$ is a direct substrate of the insulin receptor tyrosine kinase (3). Furthermore, the interaction of IRS-1 with pp125$^{FAK}$ using a mammalian two-hybrid system or coimmunoprecipitation and extensive IRS-1 tyrosine phosphorylation upon expression of pp125$^{FAK}$ in 293 EBNA cells were described (27).

Therefore, we studied the effect of neutralizing anti-pp125$^{FAK}$ antibody on PIG-dependent tyrosine phosphorylation and glucose transport activation. The inhibitory activity of this antibody was verified in an immune complex kinase assay with the substrate paxillin, the tyrosine phosphorylation of which was reduced by 70% (Table 4). The specificity of the anti-pp125$^{FAK}$ antibodies used for neutralization as well as immunoprecipitation (in subsequent experiments [see below]) was demonstrated by the very modest inhibition and precipitation, respectively, of the closely related pp116$^{PYK2}$ kinase and by their complete failure to do this with different members of the Src kinase family (Table 2). Introduction of this antibody into isolated rat adipocytes by electroporation led to an almost 50% reduction (compared to a nonrelated control IgG) in PIG 41-induced tyrosine phosphorylation of pp125$^{FAK}$ and one of its substrates, the cytoskeletal protein paxillin (4, 6, 53, 62). This was nicely correlated with inhibition of IRS-1 tyrosine phosphorylation and glucose transport upregulation in response to PIG 41 (Table 4). In contrast, basal and insulin-dependent IRS-1 tyrosine phosphorylation and glucose transport activation were not significantly affected by the anti-pp125$^{FAK}$ antibody, although it reduced pp125$^{FAK}$ and paxillin tyrosine phosphorylation in response to insulin up to 50% (Table 4). Thus, pp125$^{FAK}$ is also involved (directly or indirectly) in PIG-triggered tyrosine phosphorylation of IRS-1 and downstream signaling to the glucose transport system, but does not contribute significantly to the corresponding insulin actions and basal states.

Incubation of isolated rat adipocytes with increasing concentrations of PIG compounds (Fig. 4A, left section) revealed significant increases in tyrosine phosphorylation of immunoprecipitated pp125$^{FAK}$ and paxillin in response to PIG 41 (to up to 7.9- and 11.5-fold, respectively, at 3 μM), PIG 37 (to up to 4.3- and 9.8-fold, respectively, at 3 μM), and PIG 7 (to up to 2.5- and 4.3-fold, respectively, at 3 μM [not shown in Fig. 4A]). Furthermore, PIG 41 increased the amount of IRS-1 coimmunoprecipitated with pp125$^{FAK}$ from PIG 41-treated adipocytes in a concentration-dependent fashion to up to 9.5-fold at 1 μM (corrected for different recovery of pp125$^{FAK}$ by homologous immunoblotting, Fig. 4A, right section). Tyrosine phosphorylation of pp125$^{FAK}$ and paxillin in response to PIG 1 was very modest (to up to 1.6- and 2.9-fold, respectively, at 3 μM; Fig. 4A, left section) and apparently resulted in a weak association of pp125$^{FAK}$ with IRS-1 only (to up to 2.6-fold at 3 μM; Fig. 4A, right section). The relative rankings of the various PIG compounds with regard to activation of pp125$^{FAK}$ and pp59$^{Lyn}$ parallel one another and that for IRS-1 tyrosine phosphorylation. The combined data argue for (direct or indirect) involvement of these two kinases in PIG-induced IRS tyrosine phosphorylation.

pp125$^{FAK}$ is localized at focal adhesion plaques of cultured cells and binds to a number of proteins involved in the organization of the cytoskeleton (e.g., paxillin) and to signaling molecules, resulting in the formation of multicomponent complexes which cooperate in both the adhesion-mediated and growth-factor-mediated signaling pathways and finally initiate anchorage-dependent growth (23, 63, 76). Interestingly, pp125$^{FAK}$ as a point of convergence for both pathways has been demonstrated in Rat-1 embryo fibroblasts overexpressing the insulin receptor and Hep-G2 hepatocytes upon insulin challenge to be dephosphorylated in the adherent cells but phosphorylated in nonadherent cells (3, 24, 44). These data prompted us to investigate the influence of the cell architecture on phosphorylation and activation of pp125$^{FAK}$ in cultured 3T3-L1 adipocytes which have been incubated with increasing concentrations of PIG 41 in either an adherent or nonadherent state (see Materials and Methods). Tyrosine phosphorylation of immunoprecipitated pp125$^{FAK}$ and paxillin and coimmunoprecipitation of IRS-1 with pp125$^{FAK}$ in re-

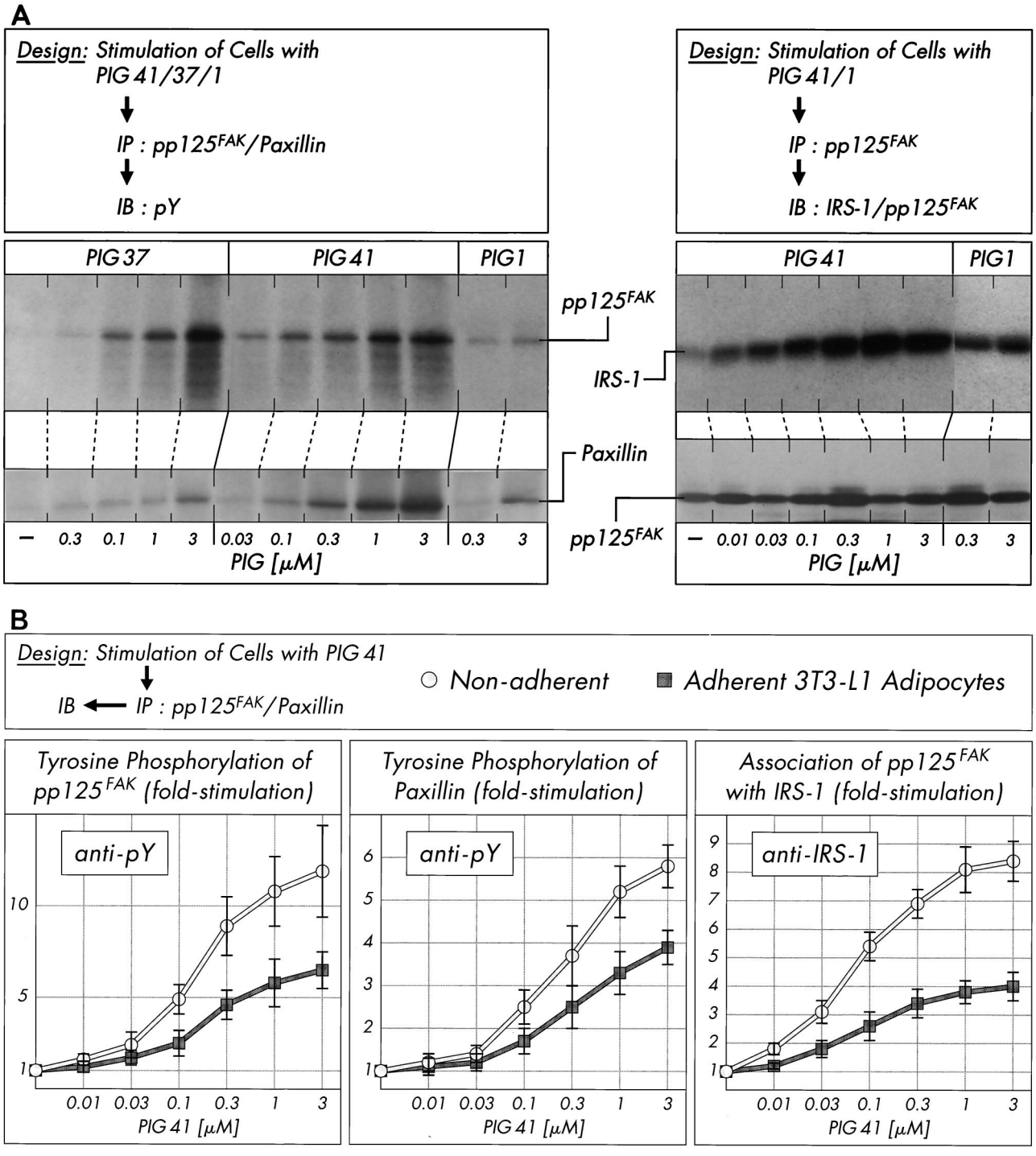


FIG. 4. Effect of PIG compounds on tyrosine phosphorylation of pp125$^{FAK}$ and paxillin and pp125$^{FAK}$-IRS-1 association. Isolated rat adipocytes (A) or nonadherent and adherent 3T3-L1 adipocytes (B) were incubated in the absence or presence of increasing concentrations of PIG compounds. pp125$^{FAK}$ and paxillin were immunoprecipitated (IP) with corresponding antibodies from defatted cell lysates and immunoblotted (IB) with anti-IRS-1, anti-pp125$^{FAK}$ (pp125$^{FAK}$ only), or antiphosphotyrosine antibodies. Phosphorimages of typical experiments are shown (A) repeated two to four times with similar results. Quantitative evaluation is given as fold stimulation (mean ± standard deviation [B]). Basal tyrosine phosphorylation and association are set at 1 in each case.

sponse to PIG 41 was significantly elevated in nonadherent 3T3-L1 adipocytes in suspension and roughly comparable to that observed with isolated rat adipocytes (Fig. 4B) compared to cells adherent on culture dishes. The maximal responses were reduced by 55% for pp125$^{FAK}$ tyrosine phosphorylation, 35% for paxillin tyrosine phosphorylation, and 50% for pp125$^{FAK}$-IRS-1 association in adherent versus nonadherent 3T3-L1 adipocytes (Fig. 4B). Next we studied whether nonadherent 3T3-L1 adipocytes loose their responsiveness to PIG upon readhesion to (fibronectin coated) culture dishes. Inhi-

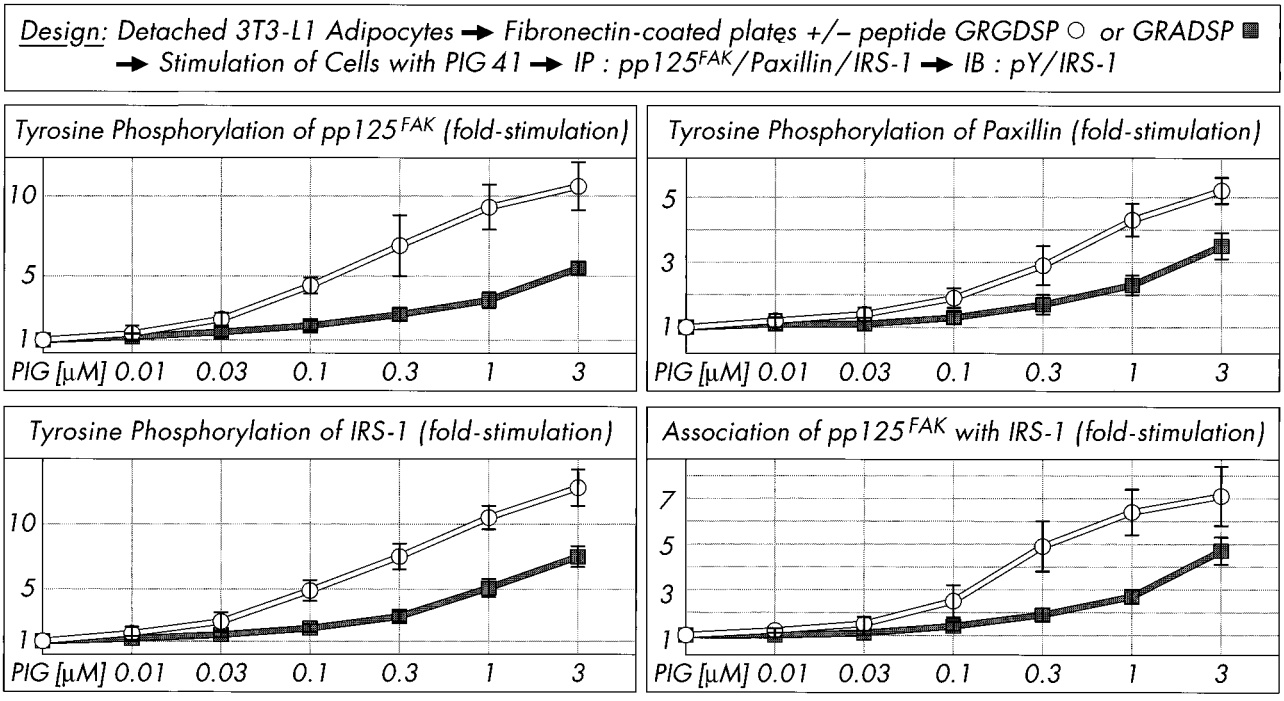


FIG. 5. Effect of cell attachment on PIG-induced tyrosine phosphorylation of pp125$^{FAK}$, paxillin and IRS-1, and pp125$^{FAK}$ and IRS-1 association. Serum-starved adherent 3T3-L1 adipocytes were detached, held in suspension (30 min), and then stimulated (10 min) in the absence or presence of increasing concentrations of PIG 41, replated on fibronectin-coated culture dishes in the absence or presence of 0.5 mM GRGDSP or GRADSP peptide, and further incubated (20 min). pp125$^{FAK}$, paxillin, and IRS-1 were immunoprecipitated (IP) with corresponding antibodies from defatted cell lysates and then immunoblotted (IB) with antiphosphotyrosine or anti-IRS-1 antibodies (pp125$^{FAK}$ only). Phosphorimages of three to four independent experiments were quantitatively evaluated as fold stimulation (mean ± standard deviation). Basal tyrosine phosphorylation and association are set at 1 in each case.

bition of adhesion of the detached 3T3-L1 adipocytes to fibronectin-coated dishes in the presence of excess RGD motif-containing peptide, GRGDSP, which specifically interferes with the integrin-fibronectin interaction, led to almost full maintenance of the maximal PIG response and sensitivity of tyrosine phosphorylation of pp125$^{FAK}$, paxillin, and IRS-1 (Fig. 5). In contrast, readhesion of the 3T3-L1 adipocytes to fibronectin-coated dishes in the presence of the nonfunctional GRADSP peptide (which fails to bind to integrins) caused a 40 to 60% reduction in PIG action. Thus, cell adhesion (presumably via the integrin-fibronectin interaction) apparently interferes with PIG-induced pp125$^{FAK}$ activation and downstream signaling in 3T3-L1 adipocytes.

**Interaction of pp125$^{FAK}$ and pp59$^{Lyn}$ in insulin-mimetic signaling and action in adipocytes.** It is generally assumed that pp125$^{FAK}$ activates Src-class kinases by docking of the phosphorylated tyrosine 397 of pp125$^{FAK}$ to the SH2 domain of the Src-class kinase, thereby preventing its carboxy-terminal phosphotyrosine residue from binding to the SH2 domain, which is assumed to keep the kinase in the inactive state (10, 47, 52). The involvement of pp125$^{FAK}$ on pp59$^{Lyn}$ regulation during PIG signaling was studied by electroporation of rat adipocytes with excess of functional Src docking site peptide (encompassing residues 385 to 405, including Y397 from the amino acid sequence of human pp125$^{FAK}$) or nonfunctional Src docking site peptide (with F397 replacing Y397) or an unrelated peptide (encompassing residues 368 to 388 from pp125$^{FAK}$) prior to treatment with PIG 41 (Fig. 6). The immune complex kinase assay with pp59$^{Lyn}$ revealed that the Src docking site peptide Y397 diminished PIG 41-induced tyrosine phosphorylation of pp59$^{Lyn}$, IRS-1, and enolase to 15 to 45% of that observed with the mutant peptide F397 or the unrelated peptide. Substrate phosphorylation by pp59$^{Lyn}$ was more susceptible to inhibition by the Src docking site peptide Y397 than autophosphorylation (Fig. 6). In conclusion, the functional Src docking site peptide functions as a potent inhibitor for pp59$^{Lyn}$ activation by PIG, most likely by preventing the interaction between pp125$^{FAK}$ and pp59$^{Lyn}$.

Consequently, we next studied the impact of blockade of the pp125$^{FAK}$-pp59$^{Lyn}$ interaction on signaling and metabolic steps downstream of pp59$^{Lyn}$. Src docking site peptide Y397 introduced into isolated rat adipocytes drastically reduced tyrosine phosphorylation of IRS-1 in response to PIG 41 (at each concentration studied), whereas nonfunctional Src docking site peptide F397 and the unrelated peptide had no significant effect (Fig. 7). The 75 to 90% blockade of IRS-1 tyrosine phosphorylation was reflected in a 30 to 55% reduction in glucose transport activation only, indicating that in isolated rat adipocytes, robust glucose transport stimulation requires modest tyrosine phosphorylation of IRS-1 only. Taken together, these findings confirm the involvement of pp125$^{FAK}$ and pp59$^{Lyn}$ in and their direct interaction (via Y397 of pp125$^{FAK}$ and SH2 of pp59$^{Lyn}$) during PIG signaling.

The sequence of pp125$^{FAK}$ contains the twin tyrosines 576 and 577, which are localized in the regulatory loop of its kinase domain and are phosphorylated by Src-class kinases both in vitro and in vivo (7). Regulatory loop peptide encompassing residues 568 to 582 from the amino acid sequence of human pp125$^{FAK}$ introduced into isolated rat adipocytes by electroporation significantly reduced PIG-dependent stimulation of tyrosine phosphorylation of pp125$^{FAK}$ (by 65 to 75%) and total IRS-1 (data not shown) as well as IRS-1 coimmunoprecipitated with the immunoprecipitated pp125$^{FAK}$ (by 50 to 65%) compared to that of a mutant control peptide containing phe-

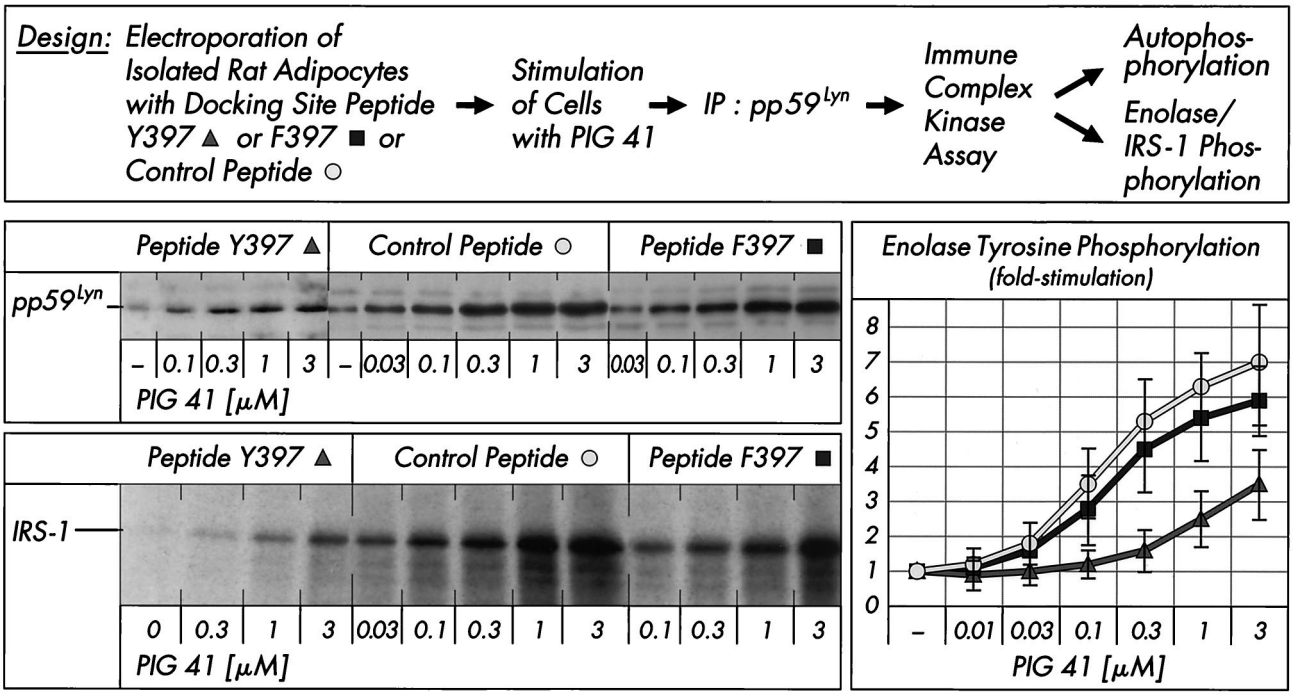


FIG. 6. Effect of pp125$^{FAK}$-Src docking site peptide on PIG-induced activation of pp59$^{Lyn}$. Isolated rat adipocytes were electroporated with control peptide, mutant Src docking site peptide F397, or wild-type Src docking site peptide Y397 (25 μg/ml) and then incubated in the absence or presence of increasing concentrations of PIG 41. pp59$^{Lyn}$ was immunoprecipitated (IP) with anti-pp59$^{Lyn}$ antibody from defatted cell lysates and then subjected to an immune complex kinase assay for autophosphorylation (by incubation with [$^{32}$P]ATP and subsequent SDS-PAGE of the total incubation mixture) or substrate phosphorylation (by incubation with unlabeled ATP and either enolase or recombinant IRS-1 and subsequent immunoblotting of the total incubation mixture with antiphosphotyrosine antibody). Phosphorimages of a typical experiment are shown (for pp59$^{Lyn}$ and IRS-1 [left section]) repeated three times with similar results. The basal pp59$^{Lyn}$ autophosphorylation in the presence of the mutant Src docking site peptide F397 was comparable to that for the control peptide (which is shown) only. Phosphorimages of enolase tyrosine phosphorylation were quantitatively evaluated as fold stimulation from four independent experiments (mean ± standard deviation [right section]) with basal values set at 1 in each case.

nylalanines 576 and 577 (Fig. 8). Interestingly, the PIG-induced association of IRS-1 with pp125$^{FAK}$ was not affected by the regulatory loop peptide, as demonstrated by sequential immunoprecipitation of pp125$^{FAK}$ and IRS-1 from stimulated adipocytes and subsequent immunoblotting for IRS-1. This suggests that phosphorylation of pp125$^{FAK}$ at the twin tyrosines by pp59$^{Lyn}$, which is presumably prevented by pp125$^{FAK}$ regulatory loop peptide, is required for maximal pp125$^{FAK}$ activation and tyrosine phosphorylation of IRS-1, but not for the interaction of pp125$^{FAK}$ with IRS-1.

The (sequential) arrangement of pp125$^{FAK}$, pp59$^{Lyn}$, and IRS-1 in a signaling pathway was further corroborated by analysis of the time courses for their tyrosine phosphorylation in response to PIG 41 in adipocytes (Fig. 9). PIG stimulation led to rapid initiation of tyrosine phosphorylation of pp125$^{FAK}$, subsequently of pp59$^{Lyn}$, and finally of IRS-1 in both isolated rat adipocytes (peaking at 5 to 30 min), and, with slightly accelerated kinetics, nonadherent 3T3-L1 adipocytes (peaking at 2 to 15 min). Thereafter, the tyrosine phosphorylation state of each of these proteins declined to about half-maximal values within the following 20 min of incubation, demonstrating the transient nature of activation of the pp125$^{FAK}$-pp59$^{Lyn}$-IRS-1-pathway by PIG in rat adipocytes and nonadherent 3T3-L1 adipocytes. In adherent 3T3-L1 adipocytes, tyrosine phosphorylation of pp125$^{FAK}$ and pp59$^{Lyn}$ declined within the initial 2 min of PIG incubation and then increased 10-fold within the next 30 min (Fig. 9). However, as observed with adipocytes in suspension, in adherent 3T3-L1 adipocytes, PIG-induced tyrosine phosphorylation of IRS-1 followed that of pp125$^{FAK}$ and pp59$^{Lyn}$ with about a 5- to 10-min delay. Taken together, the time courses for tyrosine phosphorylation argue for operation of pp59$^{Lyn}$ upstream of IRS-1 and downstream of pp125$^{FAK}$ within the PIG signaling pathway in adipocytes.

**Integrin engagement in PIG signaling and action in adipocytes.** pp125$^{FAK}$ can be activated by the integrin αβ heterodimeric transmembrane cell surface receptors that mediate interactions between the cell surface and the extracellular matrix (29, 45). The presence of $\beta_1$-integrin in rat adipocytes has been demonstrated previously (14). Therefore, we studied the effect of clustering of this integrin on IRS-1 tyrosine phosphorylation by PIG 41. $\beta_1$-Integrin clustering can be provoked by incubating cells with activating anti-$\beta_1$-integrin monoclonal antibody in the presence of the extracellular matrix protein fibronectin, which correlates with the activation of the integrin signaling pathway and enhancement of tyrosine phosphorylation of certain proteins (e.g., pp125$^{FAK}$) in a variety of cell types (25, 32), including isolated rat adipocytes (14).

Clustering with activating anti-$\beta_1$-integrin antibody plus fibronectin, but not with anti-$\beta_3$-integrin antibody plus poly-L-lysine, significantly reduced IRS-1 tyrosine phosphorylation in response to increasing concentrations of PIG 41 in comparison to control incubations (Fig. 10, left section). In nonadherent 3T3-L1 adipocytes kept in suspension during clustering, anti-$\beta_1$-integrin antibody plus fibronectin diminished autophosphorylation of pp59$^{Lyn}$ to 20 to 30% of that in the absence of clustering (Fig. 10, right section). In both isolated rat adipocytes and nonadherent 3T3-L1 adipocytes, this blockade of PIG signaling by integrin engagement was completely abol-

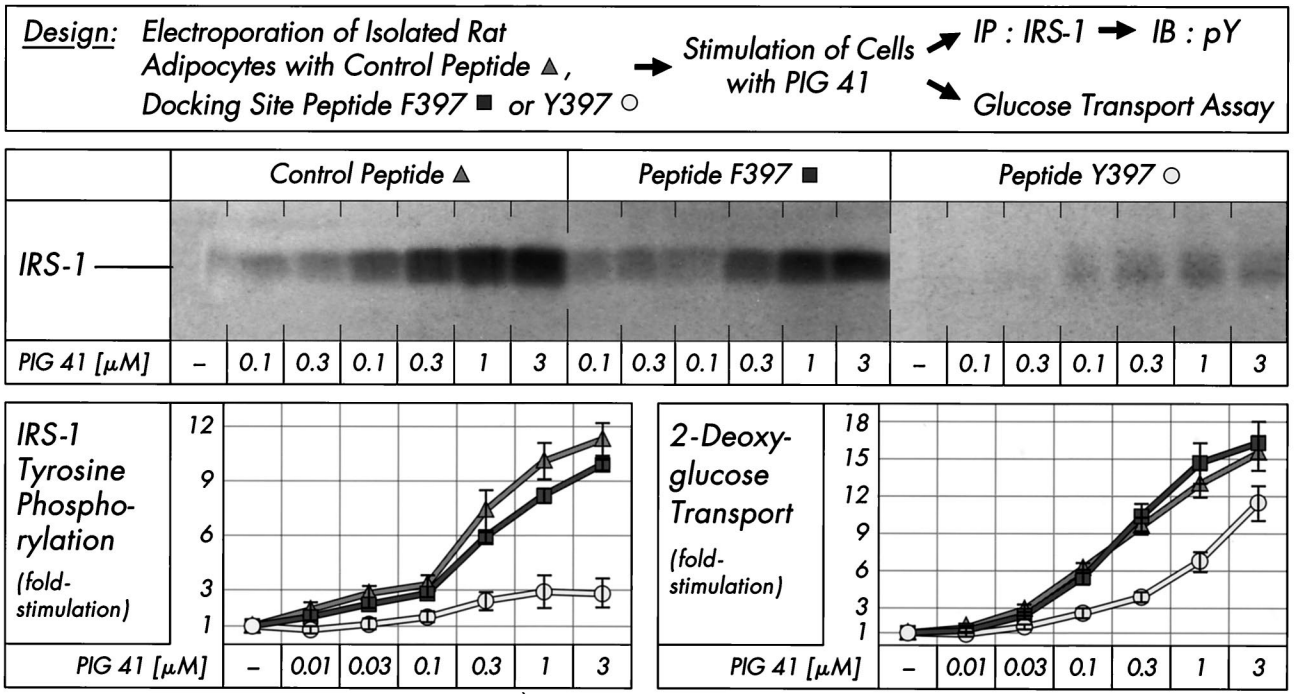


FIG. 7. Effect of pp125$^{FAK}$-Src docking site peptide on PIG-induced IRS-1 tyrosine phosphorylation and glucose transport. Isolated rat adipocytes were electroporated with control peptide, mutant Src docking site peptide F397, or wild-type Src docking site peptide Y397 (25 μg/ml) and then incubated in the absence or presence of increasing concentrations of PIG 41. IRS-1 was immunoprecipitated (IP) with anti-IRS-1 antibody from defatted cell lysates and then immunoblotted (IB) with antiphosphotyrosine antibody. Phosphorimages of a typical experiment are shown (upper section). Other portions of the cells were assayed for 2-deoxyglucose transport. Data from four independent experiments were quantitatively evaluated as fold stimulation (mean ± standard deviation), with basal values set at 1 in each case (lower section).

ished in the presence of excess of RGD motif-containing peptide, GRGDSP, but not of control peptide, GRADSP (shown for rat adipocytes, only). This GRGDSP peptide-mediated restoration of PIG-induced IRS-1 and pp59$^{Lyn}$ tyrosine phosphorylation in the presence of anti-$\beta_1$-integrin antibody plus fibronectin confirms the specificity of the inhibition of PIG signaling by integrin engagement in adipocytes in suspension.

Finally, the impact of the apparent antagonism in activation of the pp125$^{FAK}$-pp59$^{Lyn}$ pathway by integrin engagement and PIG signaling on PIG-stimulated glucose transport was studied. Incubation of isolated rat adipocytes and nonadherent 3T3-L1 adipocytes with anti-$\beta_1$-antibody plus fibronectin, but not anti-$\beta_3$-antibody plus poly-L-lysine, impaired 2-deoxyglucose transport stimulation upon challenge with increasing concentrations of PIG 41 by up to 50 to 70% in comparison to a control incubation (Fig. 11). Strikingly, in adherent 3T3-L1 adipocytes, PIG-induced glucose transport activation was not significantly affected by $\beta_1$-integrin clustering.

## DISCUSSION

In mammals, there is a clear functional distinction between insulin receptors and other members of the protein tyrosine kinase family. Whereas insulin receptors regulate metabolic pathways—e.g., the translocation of the glucose transporter isoform 4 (GLUT4) from tubulovesicular structures of the *trans*-Golgi network to the plasma membrane in muscle and adipose tissue (9)—all other receptor or non-receptor tyrosine kinases so far identified appear to control cell growth and differentiation. Consequently, the question arises of whether this specificity reflects a strict heterogeneity of the intracellular signaling pathways or whether it is the expression and the selectivity of the kinases alone that determine cellular responses (43). If the latter possibility were true, one would expect that other tyrosine kinases could mimic the metabolic effects of insulin in cells equipped with an insulin-sensitive GLUT4 translocation apparatus and concomitantly expressing the respective tyrosine kinase. This assumption has been verified in some cases, but not in others (17). Many signaling components and processes are shared by both insulin and growth factors in insulin-sensitive cells, yet their actions differ. For instance, the PDGF receptor tyrosine kinase manages to phosphorylate IRS-1 at tyrosine residues in 3T3-L1 adipocytes, which, however, does not correlate with increased glucose transport (18, 73). There are numerous examples of positive cross talk from receptors other than the insulin receptor feeding into the IRS-1–PI 3K pathway, including the G protein-coupled receptors for angiotensin and endothelin (26, 65, 66, 74); the cytokine receptors for interferons, interleukins, and tumor necrosis factor alpha (1, 69, 70, 75); the growth factor receptors for PDGF and IGF-1 (17, 41, 50); and transmembrane cell adhesion molecules, such as the integrins (54, 68). However, only in rare cases have the tyrosine kinases directly feeding into the IRS-1–PI 3K pathway and their mode of regulation been elucidated.

In the present study, we identified the non-receptor tyrosine kinases, pp125$^{FAK}$ and pp59$^{Lyn}$, and $\beta_1$-integrin as components of the PIG-dependent signaling pathway upstream of IRS-1, which upon direct interaction of the kinases induces insulin-independent stimulation of glucose transport in adipocytes. This conclusion is based on the following findings. (i) The insulin-mimetic metabolic activity of structurally different PIG compounds correlates well with their ability to induce tyrosine phosphorylation of pp125$^{FAK}$ (Fig. 4), its substrate paxillin

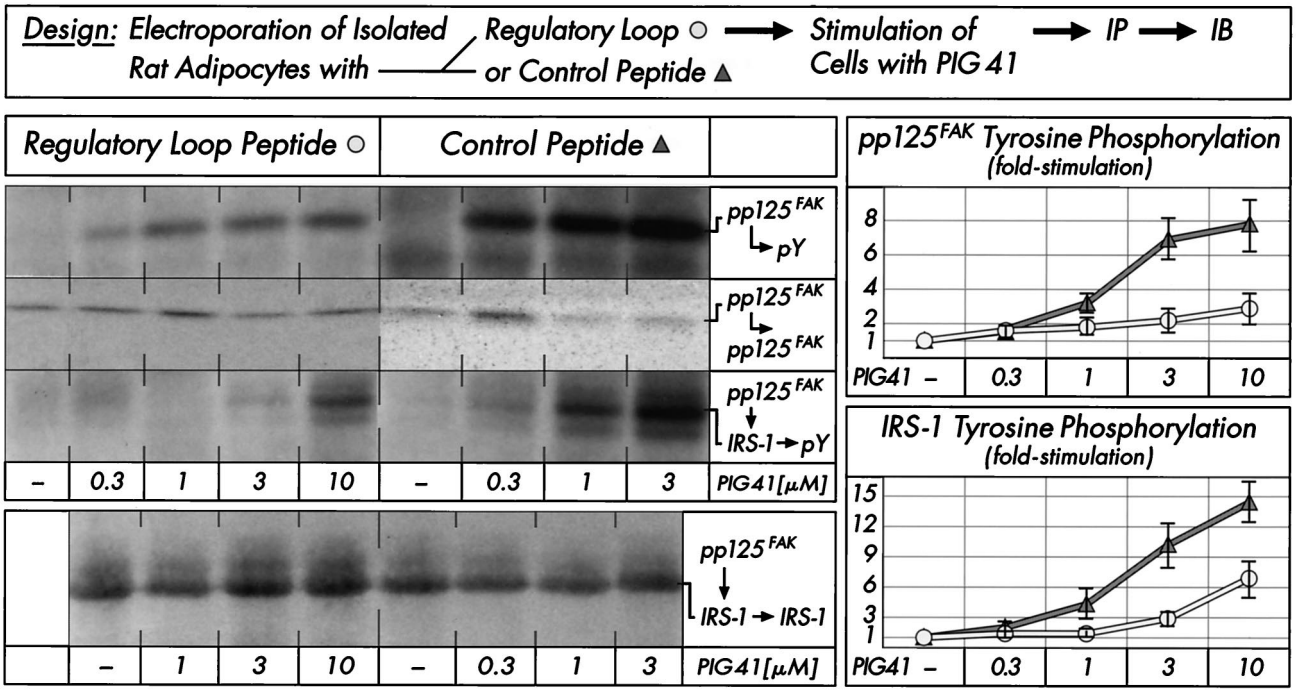


FIG. 8. Effect of pp125$^{FAK}$ regulatory loop peptide on PIG-induced tyrosine phosphorylation of pp125$^{FAK}$ and associated IRS-1. Isolated rat adipocytes were electroporated with regulatory loop peptide Y576/577 or control peptide F576/577 (50 μg/ml) and then incubated in the absence or presence of increasing concentrations of PIG 41. pp125$^{FAK}$ was immunoprecipitated (IP) with anti-pp125$^{FAK}$ antibody from defatted cell lysates and then either immunoblotted (IB) with antiphosphotyrosine or anti-pp125$^{FAK}$ antibodies or reimmunoprecipitated with anti-IRS-1 antibody as indicated. Immunoprecipitated IRS-1 was immunoblotted with antiphosphotyrosine or anti-IRS-1 antibodies. Phosphorimages of a typical experiment are shown (left section) repeated three times with similar results. Quantitative evaluation is given as fold stimulation (mean ± standard deviation [right section]). Basal tyrosine phosphorylation is set at 1 in each case.

(Fig. 4), and IRS-1 (Fig. 3B), as well as autophosphorylation of pp59$^{Lyn}$ (Fig. 3A). (ii) Introduction into isolated adipocytes of antibodies which potently inhibit pp59$^{Lyn}$ (Fig. 2) and pp125$^{FAK}$ kinase activities (Table 4) as well as of the functional Src docking site and regulatory loop peptides derived from pp125$^{FAK}$ (Fig. 7 and 8) drastically impairs PIG-dependent IRS-1 tyrosine phosphorylation and glucose transport: the former peptide by direct interference with downstream signaling to pp59$^{Lyn}$ (Fig. 6), the latter by direct inhibition of full activation of pp125$^{FAK}$ (Fig. 7). (iii) The time courses for PIG-dependent activation of pp125$^{FAK}$ and pp59$^{Lyn}$ are similar in shape to that for tyrosine phosphorylation of IRS-1, peaking in sequential order (Fig. 8). (iv) The PIG-dependent tyrosine phosphorylation of pp125$^{FAK}$ and of pp125$^{FAK}$-associated IRS-1 is more pronounced in nonadherent than in adherent 3T3-L1 adipocytes (Fig. 4B and 5). (v) $\beta_1$-Integrin clustering blocks PIG-dependent pp59$^{Lyn}$ autophosphorylation, IRS-1 tyrosine phosphorylation, and glucose transport (Fig. 10 and 11).

These results are compatible with the following model: PIG compounds trigger activation of pp125$^{FAK}$, which is antagonized by integrin engagement. Phosphotyrosine 397 of activated and autophosphorylated pp125$^{FAK}$ docks to the SH2 domain of pp59$^{Lyn}$, which is thereby activated. pp59$^{Lyn}$ phosphorylates pp125$^{FAK}$ at the tyrosines 576 and 577 within its regulatory loop, which is a prerequisite for tyrosine phosphorylation of IRS-1 associated with pp125$^{FAK}$. Thus, pp125$^{FAK}$ may act as a common signaling platform for pp59$^{Lyn}$ and IRS-1, from which the metabolic signal (e.g., to the glucose transport system) originates.

Apparently the mechanisms for pp125$^{FAK}$ activation operating during cell adhesion-integrin clustering and PIG action differ fundamentally. The inhibition of PIG signaling in response to simultaneous integrin engagement may be explained by some conformational or allosteric interference at pp125$^{FAK}$ directly or at components located upstream, including the integrins. Integrins interact with extracellular matrix proteins, such as fibronectin and vitronectin. So far we have not obtained any experimental evidence for binding of a radiolabeled PIG derivative to recombinant $\beta_1$-integrin in vitro by using either a binding assay or immunoprecipitation with anti-$\beta_1$-antibody (N. Hanekop and G. Müller, unpublished data). However, during studies of inactivation and reconstitution of isolated rat adipocytes for PIG action, we previously identified an *N*-ethylmaleimide-, trypsin-, and salt-sensitive component in the plasma membrane, which is required for PIG-induced tyrosine phosphorylation of IRS-1 and glucose transport activation (40). This 115-kDa polypeptide specifically interacts with PIG 41 (M. Gerl, M. Quint, and G. Müller, unpublished data) and presumably acts as a PIG receptor which may transmit the PIG signal across the plasma membrane or along the cell surface to $\beta_1$-integrin by a mechanism which we are currently investigating (37, 38). This molecular mode of PIG action differs strikingly from the classical view of transport of PIG-like molecules across the plasma membrane into the cytosol, where they act as allosteric activators or inhibitors of insulin-regulated enzymes of glucose metabolism (21). We were unable to measure specific uptake of a radiolabeled PIG derivative into isolated rat adipocytes (C. Piossek and G. Müller, unpublished data), arguing against a direct intracellular site of PIG action.

Cell adhesion, as well as PIG action, leads to tyrosine phosphorylation of IRS-1 to almost the full insulin response in both isolated rat adipocytes and nonadherent 3T3-L1 adipocytes

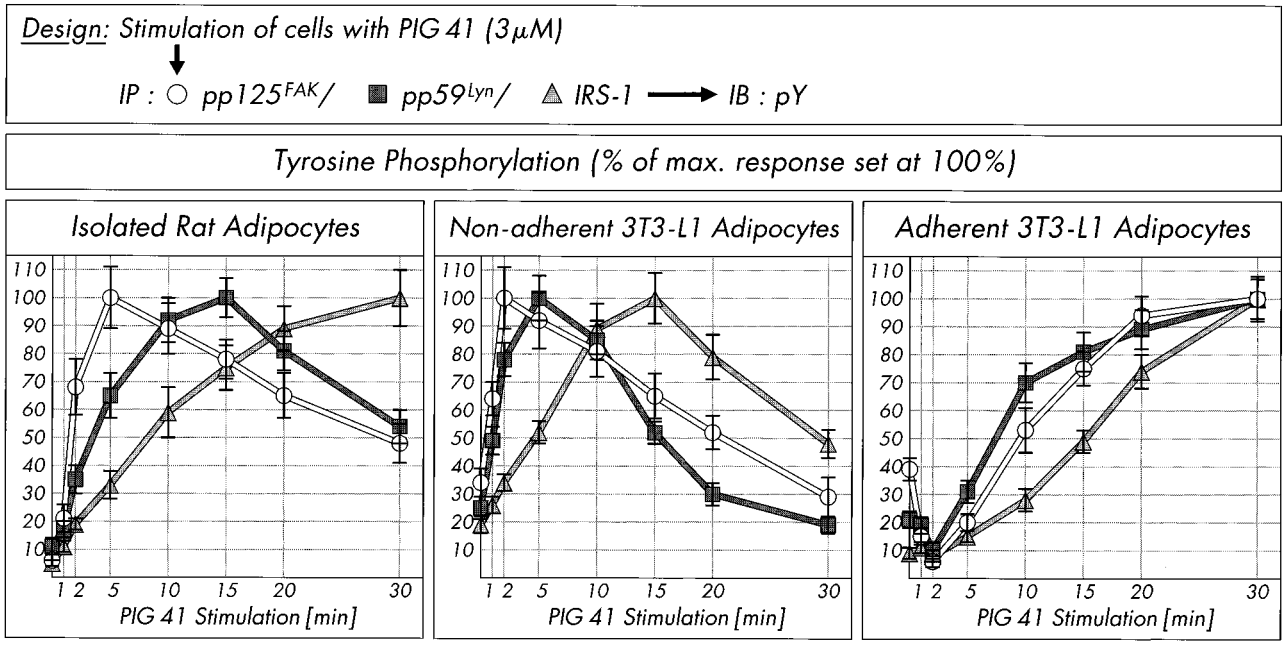


FIG. 9. Time course of PIG-induced tyrosine phosphorylation of $pp125^{FAK}$, $pp59^{Lyn}$, and IRS-1. Isolated rat adipocytes, nonadherent 3T3-L1 adipocytes, and adherent 3T3-L1 adipocytes were stimulated in the presence of 3 μM PIG 41 for various periods of time. $pp125^{FAK}$, $pp59^{Lyn}$, and IRS-1 were immunoprecipitated (IP) with corresponding antibodies from defatted cell lysates and then immunoblotted (IB) with antiphosphotyrosine antibody. Phosphorimages of three to five independent experiments were quantitatively evaluated as percentages of the control (mean ± standard deviation). Maximal tyrosine phosphorylation is set at 100% for each time course.

(14; this study). However, only PIG molecules activate glucose transport to up to 90% of the maximal insulin effect (12), whereas direct integrin clustering has no effect (14). This raises the question of how specificity is determined during PIG, insulin, and integrin signaling in adipocytes. Certainly, integrin engagement per se is not sufficient for glucose transport activation in insulin-responsive cells. The desired specificity may be based on (i) additional input(s) from a different signaling

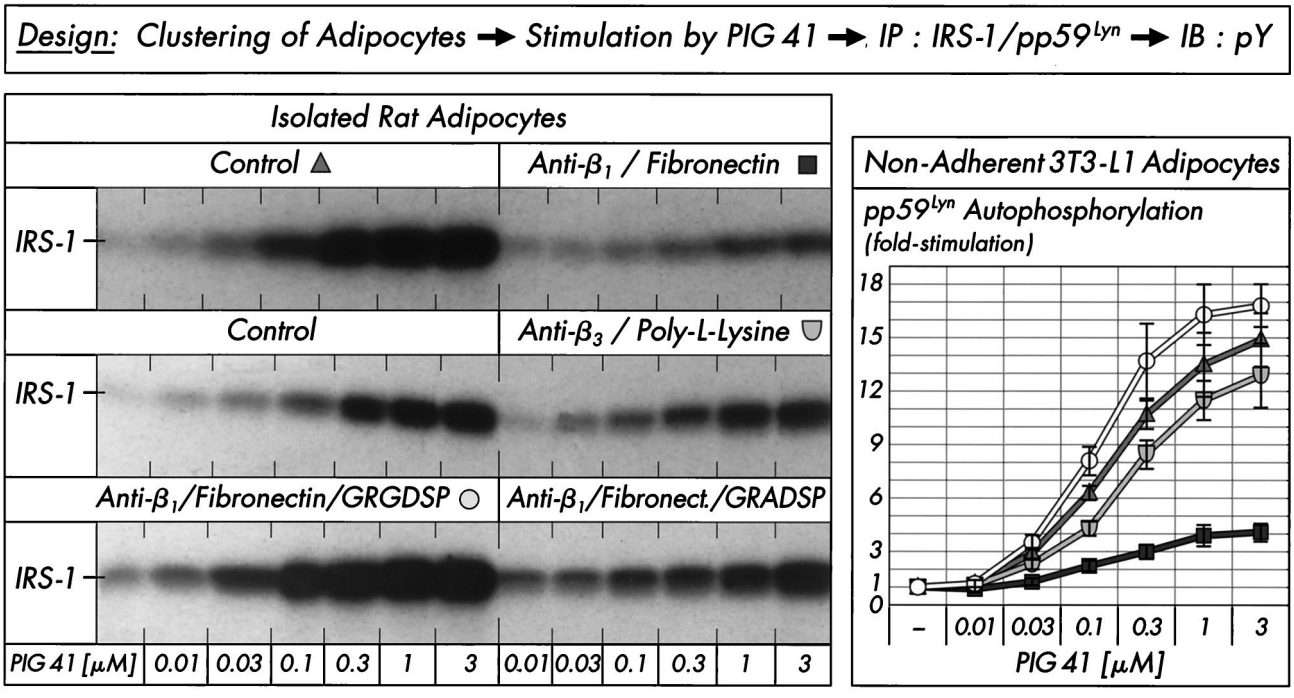


FIG. 10. Effect of integrin clustering on stimulation of IRS-1 tyrosine phosphorylation by PIG 41. Isolated rat adipocytes or nonadherent 3T3-L1 adipocytes were treated in the absence or presence of anti-$\beta_1$-integrin antibody plus fibronectin or anti-$\beta_3$-integrin antibody plus poly-L-lysine in the absence or presence of 0.5 mM GRGDSP or GRADSP peptide and then stimulated (5 min) with increasing concentrations of PIG 41. IRS-1 and $pp59^{Lyn}$ were immunoprecipitated (IP) with corresponding antibodies from defatted rat adipocyte and 3T3-L1 adipocyte lysates, respectively, and then immunoblotted (IB) with antiphosphotyrosine antibody. Phosphorimages from a typical experiment repeated three times with similar results are shown (left section) or were quantitatively evaluated from five independent experiments, respectively, as fold stimulation (mean ± standard deviation [right section]) with basal values set at 1 in each case.

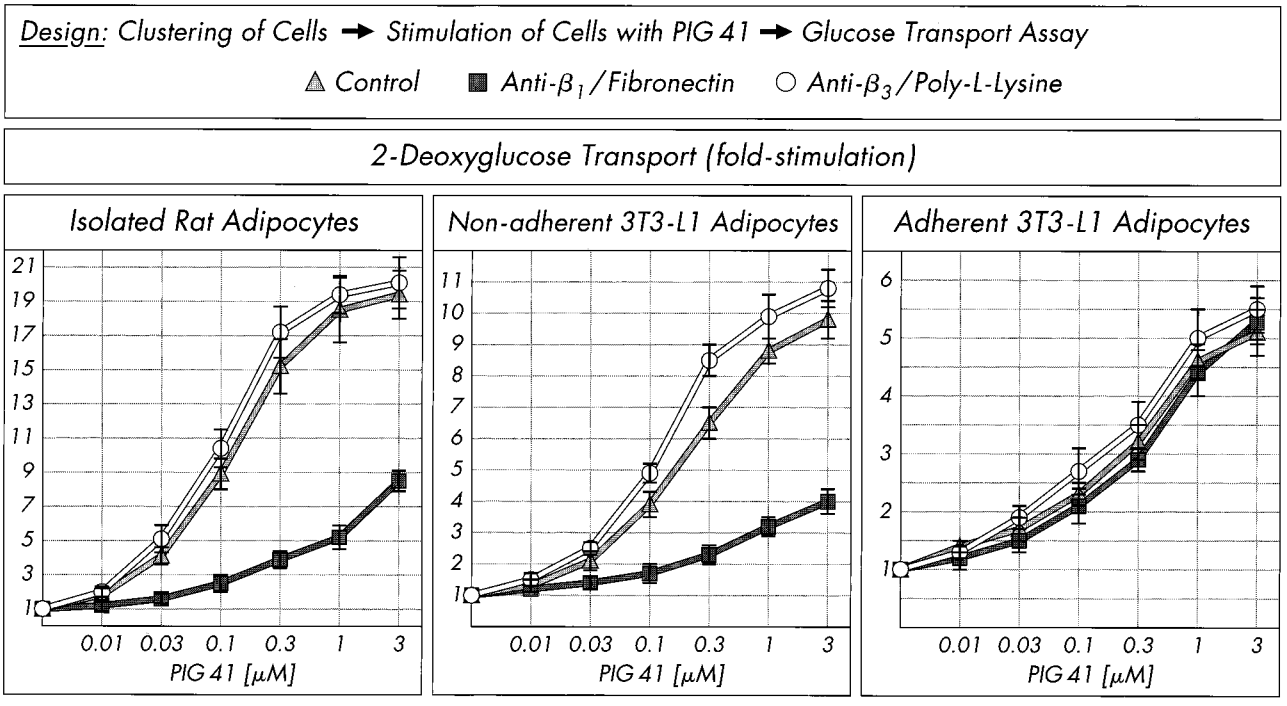


FIG. 11. Effect of integrin clustering on glucose transport activation by PIG 41. Isolated rat adipocytes, nonadherent 3T3-L1 adipocytes, or adherent 3T3-L1 adipocytes were treated in the absence or presence of anti-$\beta_1$-integrin antibody plus fibronectin or anti-$\beta_3$-integrin antibody plus poly-L-lysine and then incubated in the absence or presence of increasing concentrations of PIG 41. 2-Deoxyglucose transport was assayed and quantitatively evaluated from four independent experiments as fold stimulation (mean ± standard deviation) with basal values set at 1 in each case.

cascade which emerges from the putative PIG receptor and bypasses IRS-1 and PI 3K or (ii) different modes or kinetics of targeting or activation of IRS-1 and PI 3K. The involvement of (at least) two signals for glucose transport activation in adipocytes, one derived from the IRS-1–PI 3K pathway, and the other one unknown so far, is reminiscent of insulin action. It has been argued that insulin might differentially activate specific intracellular pools of (various isoforms of) PI 3K (41, 49). Interestingly, a cell-permeable derivative of phosphatidylinositol(3,4,5)trisphosphate, a lipid signaling product of PI 3K, was shown to stimulate glucose uptake in 3T3-L1 adipocytes treated with insulin together with the PI 3K inhibitor wortmannin, but to have no effect alone, confirming that PI 3K activation is required but not sufficient for insulin signaling to the glucose transport system (19). The insulin-mediated dissociation of the recently discovered Synip protein from VAMP2 and Syntaxin 4, the v- and t-SNAREs of the GLUT4 translocation apparatus, which thereby allows VAMP2-Syntaxin 4 interaction and final fusion of GLUT4 vesicles with the plasma membrane, may represent the PI 3K-independent signal for glucose transport activation (31). A recent report with 3T3-L1 adipocytes and L6 myotubes provided further evidence that insulin stimulates two independent signals contributing to stimulation of glucose transport with PI 3K leading to plasma membrane insertion of GLUT4 without stimulating glucose transport and a PI 3K-independent pathway involving p38 mitogen-activated protein kinase, which leads to activation of GLUT4 recruited at the cell surface (61). Apparently PIG signaling fuels both the PI 3K-dependent and PI 3K-independent pathways. Specificity may be achieved by (i) differential expression of the putative PIG receptor and/or its downstream signaling components in adipose or muscle versus non-insulin-responsive tissues and (ii) different time courses and sites for tyrosine phosphorylation of IRS proteins. The residues phosphorylated on IRS-1 in response to integrin clustering and PIG action in adipocytes have not been identified so far. Interestingly, in vitro phosphorylation of recombinant IRS-1 with $pp60^{Fyn}$ revealed a unique cohort of phosphotyrosine residues in comparison to the insulin receptor (60), arguing for differential phosphorylation of IRS-1 by non-receptor tyrosine kinases.

The physiological relevance of insulin-mimetic PIG signaling in adipocytes remains a matter of speculation so far. Adipocytes do not harbor focal adhesions (55), but they clearly express $pp125^{FAK}$ and some other components of integrin signaling, including $pp59^{Lyn}$ (rat adipocytes) and its homolog $pp60^{Fyn}$ (3T3-L1 adipocytes). Thus, the role of these kinases and their regulation by the PIG signaling cascade may be different in terminally differentiated insulin-responsive cells compared to in dividing cells. The PIG signaling cascade constituted by the PIG receptor, $\beta_1$-integrin (as a negative regulator), $pp125^{FAK}$, $pp59^{Lyn}$, and IRS-1 apparently operates as a positive cross talk to metabolic insulin signaling. We speculate that GPI proteins or PIG molecules derived thereby by lipolytic cleavage in response to certain physiological stimuli, as demonstrated recently in rat adipocytes upon insulin and glucose challenge (33), act as natural ligands for the PIG receptor. These ligands may monitor environmental situations reflecting some aspect or parameter of cell adhesion or migration (such as coordination between proliferation and differentiation and metabolic activity) different from that signaled by the extracellular matrix-integrin interaction.

## ACKNOWLEDGMENTS

We are indebted to Jochen Bauer and Andrea Bauer (Aventis Pharma Deutschland GmbH, Frankfurt am Main, Germany) for valuable support during synthesis of the PIG compounds.

## REFERENCES


1. **Argetsinger, L. S., G. W. Hsu, M. G. Myers, N. Billestrup, M. F. White, and C. Carter-Su.** 1995. Growth hormone, interferon-γ, and leukemia inhibitory factor promoted tyrosyl phosphorylation of insulin receptor substrate-1. J. Biol. Chem. **270:**14685–14692.
2. **Ashkenas, J., C. H. Damsky, M. J. Bissell, and Z. Werb.** 1994. Integrins, signaling and the remodeling of the extracellular matrix, p. 79–109. *In* D. A. Cheresh and R. P. Mecham (ed.), Integrins—molecular and biological response to the extracellular matrix. Academic Press, San Diego, Calif.
3. **Baron, V., V. Calleja, P. Ferrari, F. Alengrin, and E. Van Obberghen.** 1998. pp125$^{FAK}$ focal adhesion kinase is a substrate for the insulin and insulin-like growth factor-I tyrosine kinase receptors. J. Biol. Chem. **273:**7162–7166.
4. **Bellis, S. L., J. T. Miller, and C. E. Turner.** 1995. Characterization of tyrosine phosphorylation of paxillin in vitro by focal adhesion kinase. J. Biol. Chem. **270:**17437–17441.
5. **Brown, D. A.** 1993. The tyrosine kinase connection: how GPI-anchored proteins activate T cells. Curr. Opin. Immunol. **5:**349–354.
6. **Burridge, K., C. E. Turner, and L. H. Romer.** 1992. Tyrosine phosphorylation of paxillin and pp125$^{FAK}$ accompanies cell adhesion to extracellular matrix: a role in cytoskeletal assembly. J. Cell Biol. **119:**893–903.
7. **Calalb, M. B., T. R. Polte, and S. K. Hanks.** 1995. Tyrosine phosphorylation of focal adhesion kinase at sites in the catalytic domain regulates kinase activity: a role for Src family kinases. Mol. Cell. Biol. **15:**954–963.
8. **Clark, E. A., and J. S. Brugge.** 1995. Integrins and signal transduction pathways: the road taken. Science **268:**233–239.
9. **Czech, M. P., and S. Corvera.** 1999. Signaling mechanisms that regulate glucose transport. J. Biol. Chem. **274:**1865–1868.
10. **Eide, B. L., C. W. Turck, and J. A. Escobedo.** 1995. Identification of Tyr-397 as the primary site of tyrosine phosphorylation and pp60$^{src}$ association in the focal adhesion kinase, pp125$^{FAK}$. Mol. Cell. Biol. **15:**2819–2827.
11. **Frick, W., A. Bauer, J. Bauer, S. Wied, and G. Müller.** 1998. Insulin-mimetic signalling of synthetic phosphoinositolglycans in isolated rat adipocytes. Biochem. J. **336:**163–181.
12. **Frick, W., A. Bauer, J. Bauer, S. Wied, and G. Müller.** 1998. Structure-activity relationship of synthetic phosphoinositolglycans mimicking metabolic insulin action. Biochemistry **37:**13421–13436.
13. **Guan, J. L., and D. Shalloway.** 1992. Regulation of focal adhesion-associated protein tyrosine kinase by both cellular adhesion and oncogenic transformation. Nature **358:**690–692.
14. **Guilherme, A., and M. P. Czech.** 1998. Stimulation of IRS-1-associated phosphatidylinositol 3-kinase and Akt/protein kinase B but not glucose transport by $\beta_1$-integrin signaling in rat adipocytes. J. Biol. Chem. **273:** 33119–33122.
15. **Guilherme, A., K. Torres, and M. P. Czech.** 1998. Cross-talk between insulin receptor and integrin $\alpha_5\beta_1$ signaling pathways. J. Biol. Chem. **273:**22899–22903.
16. **Gustafson, T. A., S. A. Moodie, and B. E. Lavan.** 1998. The insulin receptor and metabolic signaling. Rev. Physiol. Biochem. Pharmacol. **137:**71–192.
17. **Huppertz, C., C. Schwartz, W. Becker, F. Horn, P. C. Heinrich, and H.-G. Joost.** 1996. Comparison of the effects of insulin, PDGF, interleukin-6, and interferon-γ on glucose transport in 3T3-L1 cells: lack of cross-talk between tyrosine kinase receptors and JAK/STAT pathways. Diabetologia **39:**1432–1439.
18. **Isakoff, S. J., C. Taha, E. Rose, J. Marcussohn, A. Klip, and E. Y. Skolnik.** 1995. The inability of phosphatidylinositol 3-kinase activation to stimulate GLUT4 translocation indicates additional signaling pathways are required for insulin-stimulated glucose uptake. Proc. Natl. Acad. Sci. USA **92:**10247–10251.
19. **Jiang, T., G. Sweeney, M. T. Rudolf, A. Klip, A. Traynor-Kaplan, and R. Y. Tsien.** 1998. Membrane-permeant esters of phosphatidylinositol 3,4,5-triphosphate. J. Biol. Chem. **273:**11017–11024.
20. **Jones, D. R., and I. Varela-Nieto.** 1998. The role of glycosyl-phosphatidylinositol in signal transduction. Int. J. Biochem. Cell Biol. **30:**313–326.
21. **Jones, D. R., and I. Varela-Nieto.** 1999. Diabetes and the role of inositol-containing lipids in insulin signaling. Mol. Med. **5:**505–514.
22. **Kessler, A., G. Müller, S. Wied, A. Crecelius, and J. Eckel.** 1998. Signalling pathways of an insulin-mimetic phosphoinositolglycan-peptide in muscle and adipose tissues. Biochem. J. **330:**277–286.
23. **Knight, J. B., K. Yamauchi, and J. E. Pessin.** 1995. Divergent insulin and platelet-derived growth factor regulation of focal adhesion kinase (pp125$^{FAK}$) tyrosine phosphorylation, and rearrangement of actin stress fibers. J. Biol. Chem. **270:**10199–10203.
24. **Konstantopoulos, N., and S. Clark.** 1996. Insulin and insulin-like growth factor-1 stimulate dephosphorylation of paxillin in parallel with focal adhesion kinase. Biochem. J. **314:**387–390.
25. **Kornberg, L., H. S. Earp, T. J. Parsons, M. Schaller, and R. L. Juliano.** 1992. Cell adhesion or integrin clustering increases phosphorylation of a focal adhesion-associated tyrosine kinase. J. Biol. Chem. **267:**23439–23442.
26. **Kowalski-Chauvel, A., L. Pradayrol, N. Vaysse, and C. Seva.** 1996. Gastrin stimulates tyrosine phosphorylation of insulin receptor substrate 1 and its association with Grb2 and the phosphatidylinositol 3-kinase. J. Biol. Chem. **271:**26356–26361.
27. **Lebrun, P., I. Mothe-Satney, L. Delahaye, E. Van Obberghen, and V. Baron.** 1998. Insulin receptor substrate-1 as a signaling molecule for focal adhesion kinase pp125$^{FAK}$ and pp60$^{src}$. J. Biol. Chem. **273:**32244–32253.
28. **Le Marchand-Brustel, Y., J.-F. Tanti, M. Cormont, J.-M. Ricort, T. Gremeaux, and S. Grillo.** 1999. From insulin receptor signalling to GLUT4 translocation abnormalities in obesity and insulin resistance. J. Recept. Signal Transduct. Res. **19:**217–228.
29. **Longhurst, C. M., and L. K. Jennings.** 1998. Integrin-mediated signal transduction. Cell. Mol. Life Sci. **54:**514–526.
30. **Macaulay, S. L., and R. G. Larkins.** 1990. Phospholipase C mimics insulin action on pyruvate dehydrogenase and insulin mediator generation but not glucose transport or utilization. Cell. Signal. **2:**9–19.
31. **Min, J., S. Okada, M. Kanzaki, J. S. Elmendorf, K. J. Coker, B. P. Ceresa, L.-J. Syu, Y. Noda, A. R. Saltiel, and J. E. Pessin.** 1999. Synip: a novel insulin-regulated Syntaxin 4-binding protein mediating GLUT4 translocation in adipocytes. Mol. Cell **3:**751–760.
32. **Miyamoto, S., H. Teramoto, J. S. Gutkind, and K. M. Yamada.** 1996. Integrins can collaborate with growth factors for phosphorylation of receptor tyrosine kinases and MAP kinase activation: roles of integrin aggregation and occupancy of receptors. J. Cell Biol. **132:**1633–1642.
33. **Müller, G., E.-A. Dearey, A. Korndörfer, and W. Bandlow.** 1994. Stimulation of a glycosyl phosphatidylinositol-specific phospholipase by insulin and the sulfonylurea, glimepiride, in rat adipocytes depends on increased glucose transport. J. Cell Biol. **126:**1267–1276.
34. **Müller, G., and W. Frick.** 1999. Signalling via caveolin: involvement in the cross-talk between phosphoinositolglycans and insulin. Cell. Mol. Life Sci. **56:**945–970.
35. **Müller, G., and K. Geisen.** 1996. Characterization of the molecular mode of action of the sulfonylurea, glimepiride, at adipocytes. Horm. Metab. Res. **28:**469–487.
36. **Müller, G., K. Schubert, F. Fiedler, and W. Bandlow.** 1992. The cAMP-binding ectoprotein from *Saccharomyces cerevisiae* is membrane-anchored by glycosylphosphatidylinositol. J. Biol. Chem. **267:**25337–25346.
37. **Müller, G., S. Welte, A. Bauer, and W. Frick.** 1999. Interaction of caveolin and non-receptor tyrosine kinases as target for insulin-mimetic compounds. Diabetes **48**(Suppl. 1)**:**A219–A220. (Abstract.)
38. **Müller, G., S. Welte, S. Wied, C. Jung, and W. Frick.** 1999. Involvement of pp125$^{FAK}$ in the insulin-mimetic signaling of phosphoinositol-glycan compounds in adherent/non-adherent adipocytes. Diabetologia **42**(Suppl. 1)**:**A66. (Abstract.)
39. **Müller, G., S. Wied, A. Crecelius, A. Kessler, and J. Eckel.** 1997. Phosphoinositolglycan-peptides from yeast potently induce metabolic insulin actions in isolated rat adipocytes, cardiomyocytes, and diaphragms. Endocrinology **138:**3459–3475.
40. **Müller, G., S. Wied, C. Piossek, A. Bauer, J. Bauer, and W. Frick.** 1998. Convergence and divergence of the signaling pathways for insulin and phosphoinositolglycans. Mol. Med. **4:**299–323.
41. **Nave, B. T., R. J. Haigh, A. C. Hayward, K. Siddle, and P. R. Shepherd.** 1996. Compartment-specific regulation of phosphatidylinositol 3-kinase by platelet-derived growth factor and insulin in 3T3-L1 adipocytes. Biochem. J. **318:**55–60.
42. **Nosjean, O., A. Briolay, and B. Roux.** 1997. Mammalian GPI proteins: sorting, membrane residence and functions. Biochim. Biophys. Acta **1331:** 153–186.
43. **Nystrom, F. H., and M. J. Quon.** 1999. Insulin signalling: metabolic pathways and mechanisms for specificity. Cell. Signal. **11:**563–574.
44. **Ouwens, D. M., H. M. M. Mikkers, G. C. M. Van Der Zon, M. Stein-Gerlach, A. Ullrich, and J. A. Maassen.** 1996. Insulin-induced tyrosine dephosphorylation of paxillin and focal adhesion kinase requires active phosphotyrosine phosphatase 1D. Biochem. J. **318:**609–614.
45. **Parsons, J. T.** 1996. Integrin-mediated signalling: regulation by protein tyrosine kinases and small GTP-binding proteins. Curr. Opin. Cell Biol. **8:**146–152.
46. **Quon, M. J., M. J. Zarnowski, M. Guerre-Millo, M. de la Luz Sierra, S. I. Taylor, and S. W. Cushman.** 1993. Transfection of DNA into isolated rat adipose cells by electroporation. Biochem. Biophys. Res. Commun. **194:**338–346.
47. **Resh, M. D.** 1998. Fyn, a Src family tyrosine kinase. Int. J. Biochem. Cell Biol. **30:**1159–1162.
48. **Richardson, A., and J. T. Parsons.** 1995. Signal transduction through integrins: a central role for focal adhesion kinase? Bioessays **17:**229–236.
49. **Ricort, J. M., J. F. Tanti, E. Van Obberghen, and Y. Le Marchand-Brustel.** 1996. Differential effects of insulin and platelet-derived growth factor on phosphatidylinositol 3-kinase at the subcellular level in 3T3-L1 adipocytes. Eur. J. Biochem. **239:**17–22.
50. **Ricort, J. M., J. F. Tanti, E. Van Obberghen, and Y. Le Marchand-Brustel.** 1997. Cross-talk between the platelet-derived growth factor and the insulin signaling pathways in 3T3-L1 adipocytes. J. Biol. Chem. **272:**19814–19818.
51. **Sargiacomo, M., M. Sudol, Z. L. Tang, and M. P. Lisanti.** 1993. Signal transducing molecules and glycosyl-phosphatidylinositol-linked proteins form a caveolin-rich insoluble complex in MDCK cells. J. Cell Biol. **122:**789–807.

52. **Schaller, M. D., J. D. Hildebrand, J. D. Shannon, J. W. Fox, R. R. Vines, and J. T. Parsons.** 1994. Autophosphorylation of the focal adhesion kinase, pp125$^{FAK}$, directs SH2-dependent binding of pp60$^{src}$. Mol. Cell. Biol. **14:** 1680–1688.
53. **Schaller, M. D., and J. T. Parsons.** 1995. pp125$^{FAK}$-dependent tyrosine phosphorylation of paxillin creates a high-affinity binding site for Crk. Mol. Cell. Biol. **15:**2635–2645.
54. **Schneller, M., K. Vuori, and E. Ruoslahti.** 1997. Alphavbeta3 integrin associates with activated insulin and PDGFbeta receptors and potentiates the biological activity of PDGF. EMBO J. **16:**5600–5607.
55. **Schwartz, M. A., M. D. Schaller, and M. H. Ginsberg.** 1995. Integrins: emerging paradigms of signal transduction. Annu. Rev. Cell. Dev. Biol. **11:**549–599.
56. **Shenoy-Scaria, A. M., L. K. Timson Gauen, J. Kwong, A. S. Shaw, and D. M. Lublin.** 1993. Palmitoylation of an amino-terminal cysteine motif of protein kinases p56$^{lck}$ and p59$^{fyn}$ mediates interaction with glycosyl-phosphatidylinositol-anchored proteins. Mol. Cell. Biol. **13:**6385–6392.
57. **Shibata, H., F. W. Robinson, C. F. Benzing, and T. Kono.** 1991. Evidence that protein kinase C may not be involved in the insulin action on cAMP phosphodiesterase: studies with electroporated rat adipocytes that were highly responsive to insulin. Arch. Biochem. Biophys. **285:**97–104.
58. **Stefanova, I., V. Horejsi, I. J. Ansotegui, W. Knapp, and H. Stockinger.** 1991. GPI-anchored cell-surface molecules complexed to protein tyrosine kinases. Science **254:**1016–1019.
59. **Su, B., G. L. Waneck, R. A. Flavell, and A. L. M. Bothwell.** 1991. The glycosyl phosphatidylinositol anchor is critical for Ly-6A/E-mediated T cell activation. J. Cell Biol. **112:**377–384.
60. **Sun, X. J., S. Pons, T. Asano, M. G. Myers, E. Glasheen, and M. F. White.** 1996. The Fyn tyrosine kinase binds Irs-1 and forms a distinct signaling complex during insulin stimulation. J. Biol. Chem. **271:**10583–10587.
61. **Sweeney, G., R. Somwar, T. Ramlal, A. Volchuk, A. Ueyama, and A. Klip.** 1999. An inhibitor of p38 mitogen-activated protein kinase prevents insulin-stimulated glucose transport but not glucose transporter translocation in 3T3-L1 adipocytes and L6 myotubes. J. Biol. Chem. **274:**10071–10078.
62. **Turner, C. E.** 1998. Molecules in focus: paxillin. Int. J. Biochem. Biophys. **30:**955–959.
63. **Turner, C. E., J. R. Glenney, and K. Burridge.** 1990. Paxillin: a new vinculin-binding protein present in focal adhesions. J. Cell Biol. **111:**1059–1068.
64. **Varela-Nieto, I., Y. Leon, and H. N. Caro.** 1996. Cell signalling by inositol phosphoglycans from different species. Comp. Biochem. Physiol. **115B:**223–241.
65. **Velloso, I. A., F. Folli, X.-U. Sun, M. F. White, M. J. A. Saad, and C. R. Kahn.** 1996. Cross-talk between the insulin and angiotensin signaling systems. Proc. Natl. Acad. Sci. USA **93:**12490–12495.
66. **Verdier, F., S. Chretien, C. Billat, S. Gisselbrecht, C. Lacombe, and P. Mayeux.** 1997. Erythropoietin induces the tyrosine phosphorylation of insulin receptor substrate-2. J. Biol. Chem. **272:**26173–26178.
67. **Virkamäki, A., K. Ueki, and C. R. Kahn.** 1999. Protein-protein interaction in insulin signaling and the molecular mechanisms of insulin resistance. J. Clin. Investig. **7:**931–943.
68. **Vuori, K., and E. Ruoslahti.** 1994. Association of insulin receptor substrate-1 with integrins. Science **266:**1576–1578.
69. **Wang, L. M., A. D. Keegan, W. Li, G. E. Lienhard, S. Pacini, J. S. Gutkind, M. G. Myers, X. Sun, M. F. White, S. A. Aaronson, W. E. Paul, and J. H. Pierce.** 1993. Common elements in interleukin 4 and insulin signaling pathways in factor-dependent hematopoietic cells. Proc. Natl. Acad. Sci. USA **90:**4032–4036.
70. **Welham, M. J., L. Learmonth, H. Bone, and J. W. Schrader.** 1995. Interleukin-13 signal transduction in lymphohemopoietic cells. Similarities and differences in signal transduction with interleukin-4 and insulin. J. Biol. Chem. **270:**12286–12296.
71. **White, M. F.** 1998. The IRS-signalling system: a network of docking proteins that mediate insulin action. Mol. Cell. Biochem. **182:**3–11.
72. **White, M. F., and C. R. Kahn.** 1994. The insulin signaling system. J. Biol. Chem. **269:**1–4.
73. **Wiese, R. J., C. C. Mastick, D. F. Lazar, and A. R. Saltiel.** 1995. Activation of mitogen-activated protein kinase and phosphatidylinositol 3′-kinase is not sufficient for the hormonal stimulation of glucose uptake, lipogenesis, or glycogen synthesis in 3T3-L1 adipocytes. J. Biol. Chem. **270:**3442–3446.
74. **Wu-Wong, J. R., C. E. Berg, J. Wang, W. J. Chiou, and B. Fissel.** 1999. Endothelin stimulates glucose uptake and GLUT4 translocation via activation of endothelin $ET_A$ receptor in 3T3-L1 adipocytes. J. Biol. Chem. **274:** 8103–8110.
75. **Yenush, L., and M. F. White.** 1997. The IRS-signalling system during insulin and cytokine action. Bioessays **19:**491–500.
76. **Zachary, I., and E. Rozengurt.** 1992. Focal adhesion kinase (pp125$^{FAK}$): a point of convergence in the action of neuropeptides, integrins, and oncogenes. Cell **71:**891–894.